**J Nonlinear Sci manuscript No.**
(will be inserted by the editor)

# Rigorous Statistical Bounds in Uncertainty Quantification for One-Layer Turbulent Geophysical Flows

**Di Qi and Andrew J Majda**

Received: date / Accepted: date

**Abstract** Statistical bounds controlling the total fluctuations in mean and variance about a basic steady state solution are developed for the truncated barotropic flows over topography. Statistical ensemble prediction is an important topic in weather and climate research. Here the evolution of an ensemble of trajectories is considered in the statistical instability analysis and is compared and contrasted with the classical deterministic instability for the growth of perturbations in one pointwise trajectory. The maximum growth of the total statistics in fluctuations is derived relying on the statistical conservation principle of the pseudo-energy. The saturation of the statistical mean fluctuation and variance in the unstable regimes with non-positive-definite pseudo-energy is achieved by linking with a class of stable reference states and minimizing the stable statistical energy bounds. Two cases with dependence on initial statistical uncertainty and on external forcing and dissipation are compared and unified with a consistent statistical stability framework. The flow structures and statistical stability bounds are illustrated and verified by numerical simulations among a wide range of dynamical regimes, where subtle transient statistical instability exists in general with positive short-time exponential growth rate in the statistical covariance even when the pseudo-energy is positive-definite. In the various scenarios illustrated below, there are strong forward and backward cascades of energy between large and small flow scales which are estimated by the rigorous statistical bounds.

**Keywords** Statistical stability analysis · topographic barotropic equations · statistical energy conservation

## 1 Introduction

In many instances in the turbulent dynamical systems, like flows in the atmosphere and ocean, the fluid develops large-scale, coherent, and essentially two dimensional patterns [15, 17, 16, 28]. Situations of obvious importance occur when smaller-scale motions have a significant feedback and interaction with a larger-scale

Di Qi
Department of Mathematics and Center for Atmosphere and Ocean Science, Courant Institute of Mathematical Sciences, New York University, New York, NY 10012
E-mail: qidi@cims.nyu.edu

Andrew J. Majda
Department of Mathematics and Center for Atmosphere and Ocean Science, Courant Institute of Mathematical Sciences, New York University, New York, NY 10012
E-mail: jonjon@cims.nyu.edu

mean flow [10,17]. The feedback and interaction induce instability that can make the steady large-scale flow very sensitive to even small changes in perturbations. The stability theory for a time-independent steady state solution in such two-dimensional turbulent systems is of interest not only in theoretical investigations but also in many experimental and observational studies [14,28,3,16,9,2].

The classical deterministic stability analysis seeks the maximum amplitude that the growing disturbance can reach in one perturbed flow trajectory near the stationary steady state [3,6,9,17]. Rigorous bounds of the growth in one unstable flow solution have also been derived based on the nonlinear saturation of instabilities [17,29]. On the other hand, the turbulent nature of the dynamical systems characterized by a large number of positive Lyapunov exponents requires a probabilistic description for the flow state variables [28,15,12,30]. Because of the statistical ensemble prediction [1,4,5,8,13,24], it is more reasonable to investigate the growth in statistics during the evolution of a probability distribution. Linear analysis of the covariance equations shows positive growth rates in the transient state even for perturbations about a stable mean state [20,27]. Statistical stability concerns the saturation of the statistical instability in fluctuations in the final stationary state. In practice, the probability distribution can be characterized by an ensemble of trajectories and the statistical stability can be described by tracking the evolution of the statistical mean in fluctuation and the variance.

In this paper, we discuss the statistical stability theory with special attention given to the interaction between small scale eddies and a dynamically evolving large-scale mean flow. The simplest set of equations that meaningfully describes the motion in geophysical flows is given by the quasi-geostrophic barotropic equations over topography with beta-effect [28,25,17]. Canonical equilibrium based on energy and enstrophy conservation predicts a Gaussian invariant measure of the topographic barotropic model with the mean potential vorticity proportional to the mean stream function in the stable regime [17,3,6]. A set of statistical steady state solutions with a large-scale steady mean flow can be assumed based on the linear dependence of potential vorticity and stream function. One interesting question in ensemble prediction is whether the mean steady state structures can persist with perturbations from initial uncertainty (due to initial mean bias and variance) and external instabilities (due to external forcing). Unlike the deterministic nonlinear stability, the statistical stability expects an ensemble initial distribution starting near a prescribed steady state to remain near it in all the time. In particular, we hope to obtain the optimal saturation bounds on the finite amplitude growth in the statistical mean and variance of the ensemble of trajectories. This is rigorous uncertainty quantification in this context, and to our knowledge we provide the first result in the present paper.

In order to focus on the dynamics in the fluctuation components away from the mean steady state, corresponding fluctuation equations of the truncated barotropic flow are introduced to define the *pseudo-energy* [17,27]. The positive-definiteness of the pseudo-energy separates the steady state solutions into stable and unstable regimes according to the linear dependence parameter of potential vorticity and stream function. Nonlinear stability theory guarantees the stability of the stable states with minimum enstrophy [3,6,17], and here we are interested in finding the optimal estimation about the maximum increase in the statistical fluctuations in the unstable solutions. The saturation bound of the unstable state can be reached by linking it to a class of reference states in the stable regime. Especially we are interested in the dynamical evolution of the statistical mean and variance of the state variables. The total statistical pseudo-energy combining the statistics in mean fluctuation and the total variance is governed by the statistical energy conservation principle introduced in [16,18]. Then the saturation bounds in both statistical mean fluctuation and the total variance in the unstable regimes are achieved through minimization among the conserved statistical energy over the class of stable reference states using the similar idea for deterministic stability in [29].

In the structure of the paper, we begin with a brief review about the statistical features of the topographic barotropic flow in stable and unstable regimes in Section 2. The turbulent flow structures are illustrated through numerical simulations in different regimes where the statistical bounds will be derived next. First in the stable regime, equilibrium statistical mechanics [3,17] predicts a Gaussian invariant measure in the statistical steady state; while in the unstable regimes, negative coefficients in the pseudo-energy forces us to separate the system into a stable and unstable subspace. The statistical bounds for fluctuations about the stable steady state are derived in Section 3 directly following the statistical energy conservation. For the unstable regimes, the following two sections develop the statistical saturation bounds based on the kinetic energy with two classes of flow disturbances. Section 4 develops the statistical bounds subject to the initial configuration of the ensemble distribution without forcing and dissipation; and Section 5 finds the saturation bounds due to external forcing and damping effects. With some additional constraints in the forms of damping and forcing operators, it can be shown that the saturation bound can be unified in a consistent framework for the two classes of perturbations.

Additional discussion for the statistical bounds with some interesting settings with forcing on a large-scale eigenmode and with upper and lower statistical bounds using the statistical enstrophy is investigated in Section 6 as special application of the general statistical stability analysis method. Especially if we look at the eddy statistics excluding the large-scale mean flow in the enstrophy, a lower statistical bound can also be discovered together with the upper bound that could offer a tight estimation about the statistical energy band constraining the range of the varying fluctuations. Finally the results are discussed in the summary in Section 7. In addition, despite the finite saturation bounds found in the main part of the paper, Appendix A shows from transient statistical analysis that strong instability exists generally with positive growth rates in the linearized covariance equation in both the stable and unstable statistical steady state solutions.

## 2 Statistical Properties of the Truncated Barotropic Flow over Topography and the Fluctuation Equations

The model of interest here is the barotropic quasi-geostrophic flow over topography on a beta-plane [25,28,17]. We consider a finite-dimensional formulation of the barotropic system with a Galerkin projection for wavenumbers within the range $|\mathbf{k}| \leq \Lambda$. Assuming a periodic boundary condition on the domain $[-\pi, \pi] \times$

$[-\pi,\pi]$, the state variables can be expanded under the Fourier modes $a_\Lambda \equiv \mathcal{P}_\Lambda a = \sum_{1\leq|\mathbf{k}|\leq\Lambda} \hat{a}_\mathbf{k} e^{i\mathbf{k}\cdot\mathbf{x}}$. The general topographic barotropic flow is given through the truncated relative vorticity $\omega_\Lambda$ and the large-scale mean flow $U$ as

$$\frac{\partial\omega_\Lambda}{\partial t} + \mathcal{P}_\Lambda\left(\mathbf{v}_\Lambda\cdot\nabla q_\Lambda\right) + U\left(t\right)\frac{\partial q_\Lambda}{\partial x} + \beta\frac{\partial\psi_\Lambda}{\partial x} = -\mathcal{D}\left(\Delta\right)\omega_\Lambda + \mathcal{F}_\Lambda, \tag{2.1a}$$

$$\frac{dU}{dt} + \fint \frac{\partial h_\Lambda}{\partial x}\psi_\Lambda\left(t\right) = -\mathcal{D}_0 U + \mathcal{F}_0, \tag{2.1b}$$

with the divergence free velocity field $\mathbf{v}_\Lambda \equiv \nabla^\perp\psi_\Lambda = \left(-\partial_y\psi_\Lambda, \partial_x\psi_\Lambda\right)$, the potential vorticity $q_\Lambda = \omega_\Lambda + h_\Lambda$, and the relative vorticity and stream function related by $\omega_\Lambda = \Delta\psi_\Lambda$. There exists a scale separation between the small-scale eddies (2.1a) and the large-scale uniform zonal flow (2.1b). The topography $h_\Lambda$ plays the role that mediates the energy transfer between the eddies and the mean flow. In addition, the external damping and forcing effects are introduced in the general form as

$$\mathcal{D}\left(\Delta\right) = \sum_{j=0}^{L} d_j\left(-1\right)^j\Delta^j, \quad \mathcal{F}_\Lambda = \sum_{1\leq|\mathbf{k}|\leq\Lambda} \hat{F}_\mathbf{k}\left(t\right)e^{i\mathbf{k}\cdot\mathbf{x}} + \dot{W}_\mathbf{k}\hat{\sigma}_\mathbf{k}\left(t\right)e^{i\mathbf{k}\cdot\mathbf{x}}, \quad \mathcal{F}_0 = F_0 + \dot{W}_0\sigma_0\left(t\right),$$

where $L$ defines different orders of dissipation. $\mathcal{D}_0, \mathcal{F}_0$ are scalars for the damping and forcing on the uniform mean flow field $U$. We also include stochastic components in the external forcing $\mathcal{F}, \mathcal{F}_0$ to represent the unresolved small-scale effects. Importantly, the dynamics on the left hand sides of the above equations (2.1) without forcing and dissipation conserve both the *kinetic energy* $E$ and the *large-scale enstrophy* $\mathcal{E}$ [17]

$$E_\Lambda = \frac{1}{2}U^2 + \frac{1}{2}\fint\left|\nabla\psi_\Lambda\right|^2, \quad \mathcal{E}_\Lambda = \beta U + \frac{1}{2}\fint q_\Lambda^2. \tag{2.2}$$

It will be shown that these quadratic invariants have a crucial role in the analysis of nonlinear stability theory and the statistical conservation principle discussed below [16,3,6].

## 2.1 Deterministic nonlinear stability without forcing and dissipation

First we review the deterministic nonlinear stability properties [17,6,3] about the evolution of one trajectory in the inviscid system (2.1). The stability theory concerns about the perturbations of variables away from a presumed basic state. The quantities of interest are then decomposed into a *time-averaged steady mean state* (denoted by upper case letters) and the *statistical fluctuations about the mean* (denoted by lower case letters with tildes) in both large-scale zonal flow and small-scale eddies

$$\psi_\Lambda\left(\mathbf{x},t\right) = \Psi\left(\mathbf{x}\right) + \tilde{\psi}\left(\mathbf{x},t\right), \quad q_\Lambda\left(\mathbf{x},t\right) = Q\left(\mathbf{x}\right) + \tilde{\omega}\left(\mathbf{x},t\right), \quad U\left(t\right) = V + \tilde{U}\left(t\right). \tag{2.3}$$

We focus on a special set of exact solutions with linear dependence in the $Q$-$\Psi$ relation (in general, we can assume $Q$ and $\Psi$ are functionally related, $f\left(Q\right) = \Psi$ [17,6]). The linear dependence between the stream function and potential vorticity defines the exact steady state solution

$$Q_{\mu}=\mu\Psi_{\mu}=\Delta\Psi_{\mu}+h,\quad V_{\mu}=-\beta/\mu. \tag{2.4}$$

The parameter $\mu$ is taken to represent the linear dependence (that is, we take the functional $f=\mu^{-1}=\text{const.}$ in the general $Q$-$\Psi$ relation). $\mu$ thus can be viewed as the eigenvalue of the elliptic operator with associated eigenfunction given by $\Psi_{\mu}$. $V_{\mu}$ represents the large-scale mean jet flow velocity. In the northern hemisphere with $\beta>0$, a positive $\mu>0$ represents westward large-scale mean jet, and a negative $\mu<0$ represents a eastward jet. Especially for the spectral modes under Fourier basis, steady state stream function and potential vorticity modes are determined through the topographic mode $\hat{h}_{\mathbf{k}}$ in the corresponding wavenumber

$$\hat{\Psi}_{\mu,\mathbf{k}}=\frac{\hat{h}_{\mathbf{k}}}{\mu+|\mathbf{k}|^{2}},\quad \hat{Q}_{\mu,\mathbf{k}}=\frac{\mu\hat{h}_{\mathbf{k}}}{\mu+|\mathbf{k}|^{2}}. \tag{2.5}$$

With the existence of topography, in general, solvable solution exists only if $\mu$ is not eigenvalues of the Laplacian operator $\Delta$ in the non-zero topographic mode wavenumber. In this way, the nonlinear interaction in (2.1a), $\nabla^{\perp}\Psi\cdot\nabla Q$, is eliminated. Indeed, if we substitute the relations back to the original equations (2.1), it is easy to check $(V_{\mu},Q_{\mu})$ forms an exact steady state solution of the equations for any values of $\mu$.

The total kinetic energy and large-scale enstrophy in (2.2) in the steady state solution (2.4) then can be calculated as a function of the parameter $\mu$

$$\begin{aligned}E_{\mu}^{L}=&\frac{1}{2}\mu^{-2}\beta^{2}+\frac{1}{2}\sum_{1\leq|\mathbf{k}|\leq\Lambda}\left(\mu+|\mathbf{k}|^{2}\right)^{-2}|\mathbf{k}|^{2}\,|\hat{h}_{\mathbf{k}}|^{2},\\ \mathcal{E}_{\mu}^{L}=&-\mu^{-1}\beta^{2}+\frac{1}{2}\sum_{1\leq|\mathbf{k}|\leq\Lambda}\left(\mu+|\mathbf{k}|^{2}\right)^{-2}\mu^{2}|\hat{h}_{\mathbf{k}}|^{2}.\end{aligned}$$

Based on the above two quadratic invariants, one given steady state kinetic energy $E_{\mu}^{L}$ offers multiple stationary solutions with different enstrophy $\mathcal{E}_{\mu}^{L}$. Nonlinear stability theory [17,6] proves stability for the branch of solutions with $\mu>0$, where the enstrophy $\mathcal{E}_{\mu}^{L}$ is minimized given energy $E_{\mu}^{L}$ from the variational principle. With deterministic stability we would expect the perturbations $\left(\tilde{U},\tilde{\omega}\right)$ in one trajectory starting near the stable branch $(V_{\mu},Q_{\mu})$ with $\mu>0$ to remain bounded near it in all the time $t>0$, that is,

$$|\tilde{U}_{t}|^{2}+\|\tilde{\omega}_{t}\|_{2}^{2}\leq C\left(|\tilde{U}_{0}|^{2}+\|\tilde{\omega}_{0}\|_{2}^{2}\right),$$

under the $L^{2}$-norm for the eddies with some constant $C>0$. The nonlinear stability can also be explained from the conservation of the pseudo-energy in fluctuations shown later in (2.8). Especially for the large-scale mean flow in northern hemisphere, the westward jet $V_{\mu}=-\beta/\mu<0$ is stable while the eastward jet becomes unstable due to the topographic effect. On the other hand the nonlinear stability result implies nothing about the solutions in the other branches $\mu<0$. The nonlinear saturation of the unstable solution is investigated in [29] by linking it with a class of stable solutions. Rigorous upper bound in perturbations of one unstable trajectory is obtained there for their deterministic nonlinear stability bounds.

From another view point, equilibrium statistical theory [17, 6, 28] predicts that there exists one *invariant Gibbs measure* for the truncated barotropic equation (2.1) with no dissipation and forcing, which is a product of Gaussian distributions with large and small scale mean, $(V_\mu, Q_\mu)$, satisfying the linear relation in (2.4)

$$p_{\mathrm{eq}}(U,q;\mu) = C^{-1}\exp\left\{-\frac{\sigma_{\mathrm{eq}}^{-2}}{2}\left[\mu\left(U-V_\mu\right)^2+\sum_{\mathbf{k}}\left(1+\mu\left|\mathbf{k}\right|^{-2}\right)\left|\hat{q}_{\mathbf{k}}-\hat{Q}_{\mu,\mathbf{k}}\right|^2\right]\right\}, \tag{2.6}$$

with $\sigma_{\mathrm{eq}}$ defining the equilibrium energy amplitude. The invariant measure is also constructed based on the kinetic energy and enstrophy invariants. One issue about the above invariant distribution in (2.6) is still that when $\mu < 0$, the equilibrium measure becomes unrealizable and is no longer valid as an invariant measure.

### 2.2 Statistical energy conservation principle of the pseudo-energy in fluctuations

In the deterministic nonlinear stability, the evolution of perturbations in one realization of the turbulent flow trajectory is investigated. Motivated by practical statistical ensemble prediction for many situations [5, 30, 13], the statistical stability that concerns the evolution of an ensemble of trajectories using the crucial statistically conserved quantities forms another group of important questions. Especially here we ask: i) whether the statistical mean state stays near the basic steady solution in (2.4) with initial and external perturbations; and ii) how the uncertainty in the fluctuations characterized by the variance amplifies in time. In the remaining sections we focus on the statistics in the fluctuation components $\left(\tilde{U},\tilde{\omega}\right)$ in (2.3), and leave the 'tildes' and the subscripts '$\Lambda$' for Galerkin projection in these components for cleaner notation.

In deriving the fluctuation equations, we first concentrate on the linear and nonlinear interaction parts in fluctuations without the inclusion of dissipation and external forcing terms. The fluctuation equations can be derived by separating the disturbances about the steady state solution (2.4) according to the linear dependence relation

$$\begin{aligned}\frac{\partial\omega}{\partial t}+\nabla^{\perp}\psi\cdot\nabla\omega+\nabla^{\perp}\Psi_\mu\cdot\nabla\left(\omega-\mu\psi\right)&\\+U\frac{\partial}{\partial x}\left(Q_\mu+\omega\right)+V_\mu\frac{\partial}{\partial x}\left(\omega-\mu\psi\right)&=0,\end{aligned} \tag{2.7a}$$

$$\frac{dU}{dt}+\fint\frac{\partial h}{\partial x}\psi=0, \tag{2.7b}$$

with $\omega=\Delta\psi$ (see [17]). The variables $(\omega,\psi,U)$ represent the fluctuation components subtracting the steady state mean $(Q_\mu,\Psi_\mu,V_\mu)$ in (2.4) depending on the parameter $\mu$. In the first line of (2.7a), $\nabla^{\perp}\psi\cdot\nabla\omega$ is the familiar nonlinear interaction term between the fluctuation modes (this quadratic interaction conserves both energy and enstrophy and satisfies a detailed triad symmetry), and the second part $\nabla^{\perp}\Psi_\mu\cdot\nabla\left(\omega-\mu\psi\right)$ is a linear operator reflecting the steady mean flow advection (this term can be viewed as a skew-symmetric operator). Besides the advection terms, two additional effects enter the fluctuation equation due to the large-scale flow fluctuation $U$ and the rotational beta-effect as the second line in (2.7a). The first term represents the effect from the large-scale mean fluctuation $U$, which is balanced by the total topographic stress in the mean flow equation (2.7b). The second term is due to steady state mean flow advection related with the $\beta$-effect, which forms a skew-symmetric operator that conserves both energy and enstrophy.

The most important aspect of the fluctuation equation is the development of conserved quantities. Unlike the original system (2.1) that conserves both energy and enstrophy, neither the kinetic energy $E$ nor the enstrophy $\mathcal{E}$ stays conserved in the fluctuation component [17]. This is due to the additional mean steady state advection from $V_\mu$ and $\Psi_\mu$ introduced to the fluctuation equations. Nevertheless we can manage to find one quadratic invariant through these two quantities in the fluctuation part. The *pseudo-energy* is suggested as a combination of the energy and enstrophy

$$\frac{dE_\mu}{dt} \equiv 0, \quad E_\mu = \mathcal{E} + \mu E = \frac{\mu}{2} U^2 + \frac{1}{2} \fint \left( \omega^2 + \mu \left| \nabla \psi \right|^2 \right), \tag{2.8}$$

which is conserved in the fluctuation dynamics (2.7). Notice that the pseudo-energy $E_\mu$ only includes the energy in fluctuations $(E, \mathcal{E})$ subtracting the previous steady state energy $\left(E_\mu^L, \mathcal{E}_\mu^L\right)$. The fluctuation equations together with the conserved pseudo-energy are discussed in detail in [16,17].

### *2.2.1 Statistical stability in fluctuations about steady state solutions*

For statistical stability we consider the statistical formulation of the pseudo-energy $E_\mu$ for bounds in both the energy in the mean fluctuation and the second-order variance. We can decompose the fluctuation variables further into *the statistical mean state* and *the disturbance about the statistical mean* (here and after we use overbar $\bar{\bullet}$ to denote ensemble averages)

$$U = \bar{U} + U', \; \omega = \bar{\omega} + \omega', \; \psi = \bar{\psi} + \psi', \quad \overline{U'} = \overline{\omega'} = \overline{\psi'} = 0.$$

The statistical mean $\left(\bar{U}, \bar{\omega}\right)$ measures the statistical bias in the fluctuation mean from the assumed steady state solution $(V_\mu, Q_\mu)$; and the disturbance $\left(U', \omega'\right)$ is the mean zero random process with their variance describing the uncertainty in the ensemble of particles during the statistical evolution of the system. Together the statistical mean and variance calibrate the total uncertainty (instability) in the fluctuation states about a steady state solution related with $\mu$. Therefore as a combination of the energy in the mean and the variance, we introduce the notion for *statistical energy in each fluctuation mode* in the form

$$E_{\mathbf{k}}^{\mathrm{stat}} \equiv \left\langle \left| \omega_{\mathbf{k}} \right|^2 \right\rangle \equiv \left| \bar{\omega}_{\mathbf{k}} \right|^2 + \overline{\left| \omega'_{\mathbf{k}} \right|^2}, \quad E_U^{\mathrm{stat}} \equiv \left\langle U^2 \right\rangle = \bar{U}^2 + \overline{U'^2}. \tag{2.9}$$

We use $\langle \bullet \rangle$ in (2.9) to represent the statistics combining the energy in the mean and the variance. For the fluctuation component in each wavenumber mode, the variance is independent of the choice of mean steady states, $\overline{\left| \omega'_{\mathbf{k}} \right|^2} = \overline{\left| q_{\mathbf{k}} \right|^2}$; and $\bar{\omega}_{\mathbf{k}}$ is the statistical mean deviation from the steady state solution, $\bar{\omega}_{\mathbf{k}} = \bar{q}_{\mathbf{k}} - Q_{\mu,\mathbf{k}}$, thus depends on the parameter value of $\mu$. Finally we can define the ***total statistical energy***

***in fluctuations*** through the original pseudo-energy (2.8) as a combination of mean and variance

$$E_{\mu}^{\mathrm{stat}} \equiv \frac{\mu}{2} E_{U}^{\mathrm{stat}} + \frac{1}{2} \sum_{1 \leq |\mathbf{k}| \leq \Lambda} \left(1 + \mu \, |\mathbf{k}|^{-2}\right) E_{\mathbf{k}}^{\mathrm{stat}}. \tag{2.10}$$

It is useful to investigate the ensemble statistics in the first two moments rather than a single trajectory realization since they not only characterize the deviations from the steady state mean, but also illustrate the evolution of uncertainty (variance) for this mean estimation. Thus the ensemble performance offers more reasonable and detailed characterization of the system especially when it becomes increasingly turbulent.

It can be implied from the conservation of pseudo-energy (2.8) that the statistical energy $E_{\mu}^{\mathrm{stat}}$ for fluctuation is also invariant in time

$$\frac{d}{dt} E_{\mu}^{\mathrm{stat}} = 0, \tag{2.11}$$

in the case with no dissipation and external forcing. This is concluded from the symmetry in the nonlinear interactions in the fluctuation dynamics (2.7) and the linear operators are skew-symmetric with no explicit contribution to the statistical energy. Details about the conditions and derivation of the statistical energy conservation principle are discussed in [18,16]. Especially statistical nonlinear stability can be concluded from the statistical energy in fluctuation components consistent with the deterministic stability results before. The stability can be determined through the sign in the statistical energy $E_{\mu}^{\mathrm{stat}}$ spectral components (2.10) depending on the value of the parameter $\mu$:

- *Stable regime*: If $\mu > 0$, the statistical energy in fluctuation $E_{\mu}^{\mathrm{stat}}$ is uniformly positive-definite in each vortical mode and large scale mean flow $U$. The nonlinear stability about the mean and variance perturbations can be analyzed all together for the total variability from the conservation of the total statistical energy;
- *Unstable mean flow*: If $-1 < \mu < 0$, the statistical energy in the mean flow component $U$ is negative while all the other vortical modes stay positive with $1 + \mu \, |\mathbf{k}|^{-2} > 0$ for all $\mathbf{k}$. In this case, we need to separate the statistical energy into the large-scale mean flow energy $E_{U}^{\mathrm{stat}}$ and all the other smaller-scale eddy energy $E_{\omega}^{\mathrm{stat}}$ to analyze them separately;
- *Unstable regime*: If $\mu < -1$, the positive-definite property of the statistical energy in all the vortical modes is also not guaranteed. Both the mean flow $U$ and large-scale vortical modes with $1 + \mu \, |\mathbf{k}|^{-2} < 0$ become unstable. The total statistical energy needs to be decomposed into a positive-definite and negative-definite part and analyzed separately (see details in Section 4).

*Transient statistical instability with positive growth rate in the covariance among all the regimes* It needs to be emphasized that subtle statistical instability can be generated showing a large number of positive internal growth rates in general in the turbulent flow in both the statistically stable and unstable regimes above throughout all the parameter values. The variance of an ensemble of particles beginning from a Gaussian distribution could suffer strong exponential growth in the starting time from transient statistical stability analysis. See Appendix A and [17,7,14] for more details about the general large uncertainty inside the system. In the following sections, we will begin with the simple stable regime $\mu > 0$ with positive-definite statistical energy; then we will turn to the non-positive-definite regime $\mu < 0$ for energy balance between the small and large scales. Especially it is an interesting case in regime $-1 < \mu < 0$ with explicit interaction between the unstable mean flow $U$ and small-scale flow eddies through topographic stress. Next we consider the effect of external damping and forcing to the total statistical energy.

*2.2.2 Forced-dissipative case with Ekman damping and forcing*

In general the dissipation and forcing on the right hand sides of the original flow dynamics (2.1) introduce additional source and sink terms to the statistical energy dynamics. The pseudo-energy $E_\mu$ in (2.8) becomes no longer conserved, and so is the statistical fluctuation due to the pseudo-energy. For simplicity in representation we take uniform Ekman damping as the dissipation effect, that is, let $\mathcal{D} = dI$ in the general dissipation in (2.1). The Ekman damping is common in geophysical flows [17,28]. In addition we assume the deterministic forcing contains a first component from the equilibrium steady state. Therefore, on the right hand sides of the flow equations (2.1), forcing and dissipation terms are applied in the simplified form

$$\begin{aligned} \text{small scale}: &\quad -d\omega + d\bar{\omega}_{\text{eq}} + F(\mathbf{x}) + \sigma_{\mathbf{k}}\dot{W}_{\mathbf{k}}, \\ \text{large scale}: &\quad -dU + d\bar{U}_{\text{eq}} + F_0 + \sigma_0\dot{W}_0. \end{aligned} \tag{2.12}$$

Above the equilibrium mean states $\left(\bar{\omega}_{\text{eq}}, \bar{U}_{\text{eq}}\right)$ are determined from the steady state solutions in (2.5) depending on the parameter value $\mu$, $\bar{\omega}_{\text{eq},\mathbf{k}} = -\left|\mathbf{k}\right|^2 \hat{\Psi}_{\mu,\mathbf{k}}$ and $\bar{U}_{\text{eq}} = V_\mu$. Therefore linear damping is applied on the fluctuation components in both small and large scale variables $\tilde{\omega} = \omega - \bar{\omega}_{\text{eq}}, \tilde{U} = U - \bar{U}_{\text{eq}}$. We also assume additional deterministic forcing $(F, F_0)$ and stochastic white noise forcing with amplitude $(\sigma, \sigma_0)$ on both small and large scales. Accordingly the statistical energy equation with forcing and Ekman damping [16,18,27] becomes

$$\frac{dE_\mu^{\text{stat}}}{dt} = -2dE_\mu + \mu F_0 \cdot \bar{U} + \left\langle \bar{\omega}, F \right\rangle_\mu + Q_{\sigma,\mu}. \tag{2.13}$$

Above the inner product is defined through the metric in the pseudo-energy (2.10)

$$\left\langle \bar{\omega}, F \right\rangle_\mu = \sum_{1\leq|\mathbf{k}|\leq\Lambda} \left(1 + \mu\left|\mathbf{k}\right|^{-2}\right) \hat{F}_{\mathbf{k}}^* \cdot \bar{\omega}_{\mathbf{k}},$$

and the entire contribution from the stochastic white noises forcing is represented as

$$Q_{\sigma,\mu} = \frac{1}{2}\mu\sigma_0^2 + \frac{1}{2}\sum_{1\leq|\mathbf{k}|\leq\Lambda} \left(1 + \mu\left|\mathbf{k}\right|^{-2}\right) \sigma_{\mathbf{k}}^2,$$

Especially in the unstable regime $\mu < 0$, both the deterministic and stochastic forcing can introduce negative effects to the statistical energy changing rate on the right hand side of (2.13). As a further comment, only the statistical mean is included in the contribution to the total statistical energy change due to the exerted external forcing. Thus the dynamics of the total statistical energy combining mean and variance in (2.13) is determined through only the change in first order mean state together with the external forcing and dissipation effects. The statistical energy dynamical equations are formulated with detail in [18,16,27].

*Remark.* In fact, for the general dissipation form $\mathcal{D}$, we can always find a constant lower bound $C_d$ of the entire damping effect independent of wavenumber $\mathbf{k}$ as

$$C_d \equiv \sum_{j=0}^{L} d_j \leq \mathcal{D}\left(-|\mathbf{k}|^2\right) = \sum_{j=0}^{L} d_j\, |\mathbf{k}|^{2j}\,, \quad \forall\ |\mathbf{k}| \geq 1.$$

Thus the above statistical energy conservation law (2.13) just becomes a dynamical inequality

$$\frac{dE_\mu^{\text{stat}}}{dt} \leq -2C_d E_\mu + \mu \bar{U} \cdot F_0 + \langle \bar{\omega}, F \rangle_\mu + Q_{\sigma,\mu}.$$

Then the same strategy can apply for statistical stability analysis.

## 2.3 Illustration of flow structures and statistics with numerical simulations

We first illustrate the typical flow structures through direct numerical simulations in various parameter regimes where the rigorous statistical bounds will be derived in the next sections. Throughout this paper, we will always refer to the following model setup to test the statistical stability in fluctuations according to different steady state solutions and different deterministic and stochastic forcing scenarios with parameter $\mu$. A relatively small truncation size $|\mathbf{k}| \leq \Lambda = 12$ is used so that we can concentrate on the major large-scale structures while the effects of nonlinear feedbacks are also maintained. To capture the statistics in the state variables, we run a Monte-Carlo simulation of the original topographic barotropic system (2.1) with an ensemble size $N = 1000$. More numerical simulations with larger ensemble size has confirmed that $N = 1000$ is large enough to capture the essential statistical mean and variance with accuracy. For the topography, we assume a zonal structure on the largest scale mode with perturbations added in smaller scales such that

$$h = H\left(\sin x + \cos x\right) + H \sum_{2 \leq |\mathbf{k}| \leq \Lambda} |\mathbf{k}|^{-2}\, e^{i(\mathbf{k}\cdot\mathbf{x} - \theta_{\mathbf{k}})}. \tag{2.14}$$

In the simulations we take the topographic strength $H = 3\sqrt{2}/4$ and uniform phase shift $\theta_{\mathbf{k}} = \frac{\pi}{4}$. This topography structure is an analog to a long north-south ridge and has been used for various uncertain quantification problems [17,22,27,21,11]. Here the beta-effect is set as $\beta = 1$ in most of the test cases. We will mostly consider the evolution of statistical ensemble uncertainties in the following two different perturbation scenarios:

- *Model dependence on initial ensemble statistics without forcing and dissipation*: We consider the evolution of an ensemble of particles beginning with a Gaussian distribution. The initial mean of the ensemble is set the same as steady state solution $(V_\mu, Q_\mu)$ in (2.5), and uniform initial variances are introduced $\sigma_{U,0} = 1, \sigma_{\text{un},0} = 1$ but only on the mean flow $U$ and the unstable vortical modes $\hat{\omega}_{\mathbf{k}}, \mu + |\mathbf{k}|^2 < 0$. All the other modes are set with zero initial variances;

– *Model dependence on energy source and sink from external forcing and dissipation*: Linear Ekman damping with different rates $d$ as in (2.12) is used. The deterministic forcing is chosen according to the steady state solution of large and small scale variables, $\bar{U}_{\mathrm{eq}} = V_\mu$ and $\bar{\omega}_{\mathrm{eq}} = -|\mathbf{k}|^2 \hat{\Psi}_{\mu,\mathbf{k}}$, and the stochastic white noise forcing is taken with uniform amplitude only applied on the mean flow $U$ and the the unstable vortical modes. The amplitude $\sigma$ is taken so that $d^{-1}\sigma^2 = 1$.

In the first case without damping and forcing the initial statistics in fluctuation will be persistent for the entire time; while with damping and forcing the initial configuration will decay and become irrelevant in the final steady state distribution. In both cases, all statistical energy in fluctuation is injected in the unstable large scales in the beginning, and gets amplified and cascaded down to the smaller scales which contain no initial uncertainty or are not being forced. All the statistics are calculated after the model has reached the equilibrium statistical steady state.

### *2.3.1 Invariant measure and ergodicity in the statistically stable regime*

In the first place, we test the flow field with no forcing and dissipation on the right hand sides of (2.1) in the regime $\mu > 0$. Here we use the parameter value $\mu = 1$ to illustrate the flow structure in statistical steady state. From the nonlinear stability and equilibrium statistical mechanics the flow statistics will converge to the Gaussian invariant measure in (2.6) with stable mean and variance determined by the topography $h$, beta-effect $\beta$, and parameter $\mu$. Furthermore the numerical ergodicity of the system confirms that the invariant measure is unique so that the ensemble statistics in steady state (which are estimated at the final time with ensemble average) is in agreement with the time-averaged result (which are averaged along one single trajectory of the solution). To keep tracking the evolution of statistical mean and variance at the same time, we use an ensemble approximation to get the statistics in the system rather than just run a single trajectory simulation for long time averages.

In Figure 2.1 we show the snapshot of relative vorticity in fluctuation in steady state and the statistical mean stream function in final equilibrium with parameter $\mu = 1$. The relative vorticity fluctuates away from the steady state solution $Q_\mu$ and is isotropic in the spectral domain. Even in this stable regime, many small scale vortices are generated in the vorticity field due to nonlinear interactions and transient statistical growth in uncertainty (see Appendix A). Also we plot the full flow vector field including the large-scale mean flow $U$ and small-scale stream function. The mean stream function and flow field is determined by the topography and beta-effect $\mu\Psi_\mu = \Delta\Psi_\mu + h, V_\mu = -\beta/\mu$ in (2.4). A steady westward mean jet is generated as predicted from the steady state solution. The consistency in the mean flow is also shown in Table 1 for the stable regime. We will discuss the statistical bounds in fluctuation mean and variance in the stable regime $\mu > 0$ next in Section 3.

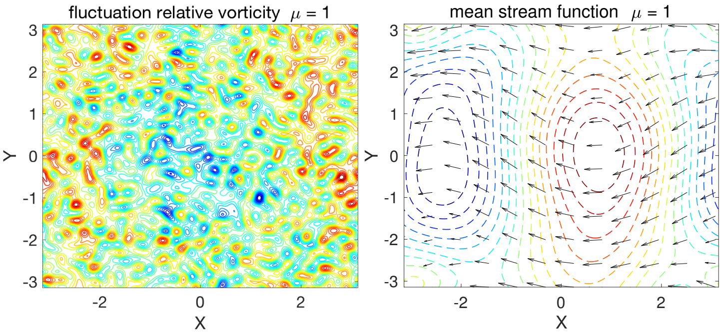


Fig. 2.1: Snapshots of the relative vorticity in fluctuation component $\tilde{\omega}$ and the statistical mean stream function $\psi$ (without the large-scale flow $U$) together with the entire flow vector field (including large-scale flow $U$) with parameter $\mu = 1$ at equilibrium steady state.

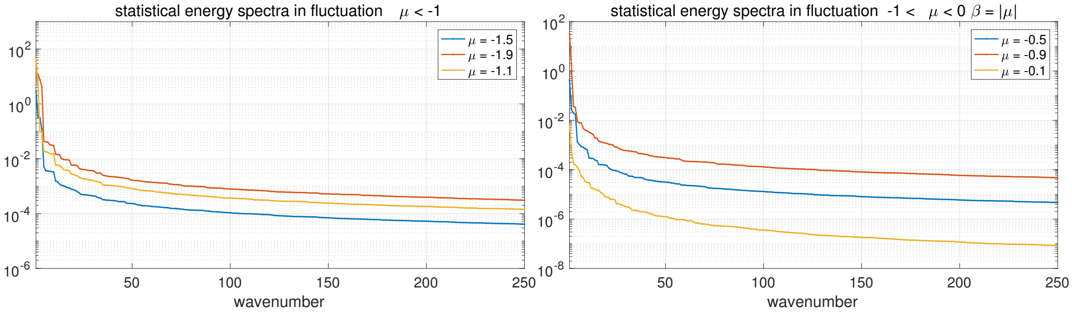


Fig. 2.2: The fluctuation statistical energy spectra for typical values of regimes $-2 < \mu < -1$ and $-1 < \mu < 0$. The modes are ordered in the descending order in energy.

### *2.3.2 Flow statistics depending on initial ensemble distribution in unstable regimes*

Next we show the statistical evolution of initial fluctuations in the two typical nonlinear unstable regimes $\mu < -1$ and $-1 < \mu < 0$ without forcing and dissipation. Especially in regime $-1 < \mu < 0$ with only the mean flow $U$ unstable, we change the beta-effect to $\beta = -\mu$ to increase the flow fluctuations near the limit $\mu \to 0$ (see Appendix A). In Figure 2.2 the statistical energy spectra in the fluctuation component at statistical steady state are compared for several typical values of $\mu$. The modes are ordered in a descending order, which in this case is basically from the largest scales to the smaller scales. In the steady spectra among values $-2 < \mu < -1$, the statistical energy in each mode with intermediate value $\mu = -1.5$ is relatively small; while in the other two cases, $\mu = -1.9$ and $\mu = -1.1$, larger statistical energy fluctuations get generated especially among the small modes in the tails. This suggests larger instability as the parameter approaches the two limits, $\mu \to -1, -2$. In the spectra of the case $-1 < \mu < 0$ the steady state statistical energy in each mode gets smaller monotonically as the parameter $\mu$ approaches zero. This implies no instability in fluctuations any more near the limit $\mu \to 0$ even though it gets a large mean steady state $V_\mu = -\beta/\mu$ from the equilibrium statistical mechanics and the invariant measure (2.6).

We show the flow structures in steady state for the test cases. Figure 2.3 compares the relative vorticity in fluctuations when the parameter values change from $\mu = -0.5, -1.1, -1.5, -1.9$. The vorticity fields in fluctuation depict the deviation from the assumed steady state flow solution $Q_\mu$. The color scales of the plots are normalized to the same range for comparison. Obviously in the vorticity field with $\mu = -1.9$ and

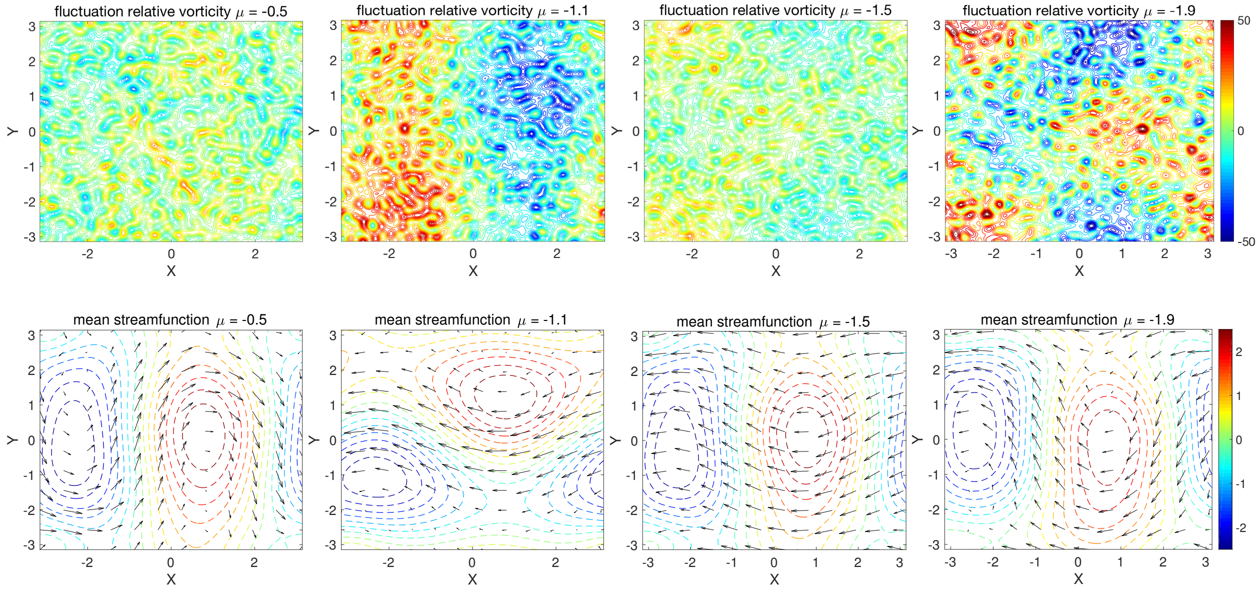


Fig. 2.3: Snapshots of the relative vorticity field in fluctuation component $\tilde{\omega}$ with parameters $\mu = -0.5$, $\mu = -1.1$, $\mu = -1.5$, and $\mu = -1.9$. The mean stream function (without mean flow $U$) and the entire flow vector field (with mean flow $U$) for the parameter values are shown in the second row.

| $\mu$ | -1.9 | -1.5 | -1.1 | -0.9 | -0.5 | -0.1 | 0.5 | 1 |
|---|---|---|---|---|---|---|---|---|
| $\bar{U}$ | -0.8222 | -2.4816 | -2.9737 | 0.3401 | 0.2282 | 0.6974 | -2.0498 | -1.1617 |
| $-\beta/\mu$ | 0.5263 | 0.6667 | 0.9091 | 1 | 1 | 1 | -2 | -1 |

Table 1: Statistical mean large-scale flow $\bar{U}$ in statistical steady state without damping and forcing compared with the assumed steady state solution $V_\mu = -\beta/\mu$.

$\mu = -1.1$, larger small-scale structures are induced with stronger fluctuations compared with the $\mu = -1.5$ and $\mu = -0.5$ cases. Notice that the initial statistics only sets the non-zero ensemble variance in the largest scales $|\mathbf{k}| = 1$, thus the vortical fluctuations in smaller scales are generated from the internal instability producing a direct cascade of enstrophy. Also we compare the statistical mean field of the stream functions and the entire flow vector field. The large-scale zonal flow shifts from a weak eastward jet ($\mu = -0.5$) to strong westward jets ($\mu < -1$) as $\mu$ decreases. Especially westward mean flow $\bar{U} < 0$ is always developed in steady state for $\mu < -1$ starting from the eastward initial state $V_\mu = -\beta/\mu > 0$ with small perturbations in the ensemble.

Besides, we list the steady state statistical mean of the large-scale flow $\bar{U}$ as the parameter $\mu$ varies in Table 1. In the stable regime $\mu > 0$, the theoretical steady state solution $V_\mu = -\beta/\mu$ gives accurate prediction in agreement with the numerical results of steady state mean flow $\bar{U}$. This implies little statistical instability in the flow field in this regime. On the other hand, with $\mu < -1$ the steady state mean flow $\bar{U}$ gets the opposite direction compared with the assumed steady state solution $V_\mu$. This implies the strong instability that adds large deviations to the mean flow field through topographic stress. In the regime $-1 < \mu < 0$, $\bar{U}$ and $V_\mu$ also have difference in value but stay in the same direction. This corresponds to the weaker instability only in the large scale flow $U$. The statistical saturation bounds for flows in the various unstable regimes without forcing and dissipation will be developed next in Section 4.

| $d$ | 0.05 | | | 0.1 | | | 0.25 | | |
|---|---|---|---|---|---|---|---|---|---|
| $\mu$ | -1.1 | -1.5 | -1.9 | -1.1 | -1.5 | -1.9 | -1.1 | -1.5 | -1.9 |
| $\bar{U}$ | 0.2326 | -0.4457 | -1.4331 | 0.4026 | -0.1213 | -1.1408 | 0.7771 | 0.2724 | -0.4737 |
| $\overline{U'^2}$ | 0.8194 | 0.3853 | 1.0750 | 1.0695 | 0.6129 | 1.7450 | 1.2188 | 0.6267 | 2.3040 |

Table 2: Statistical mean and variance in large-scale flow $U$ in statistical steady state with changing $\mu$ and damping rate $d$.

#### *2.3.3 Flow equilibrium statistics depending on external forcing and dissipation*

In the final test case we consider the effects from linear damping and forcing in the form (2.12) in the flow field as described before. Effects with different Ekman damping $d$ are considered. The deterministic forcing is first taken purely from the steady mean state, $F_0 = dV_\mu$ and $\hat{F}_{\mathbf{k}} = -d\,|\mathbf{k}|^2\,\hat{\Psi}_{\mu,\mathbf{k}}$. The the mean stream function and the entire flow vector fields including mean flow with changing values of $\mu$ are shown in Figure 2.4. Stronger forcing and damping drive the flow closer to the exact steady state solution in the equilibrium, while the weaker forcing and damping cases introduce larger fluctuations. In the steady state mean flow as the parameter $\mu$ changes, the background mean flow shifts from a eastward jet to blocked circulations and finally to a westward flow in a similar way as the previous case. Numerical simulations show a eastward jet when $\mu = -0.5$, and the eastward flow becomes weaker and finally a westward jet gets developed as $\mu$ decreases to $-1.1, -1.5, -1.9$. Table 2 lists the equilibrium mean and variance in the large-scale flow $U$ with different damping rates $d$ and parameter values $\mu$. The mean flow shifts from eastward ($\bar{U} > 0$) to westward ($\bar{U} < 0$) as $\mu$ changes from $-1$ to $-2$, and the variance increases as $\mu$ approaches near the two boundaries and stays small in the intermediate values of $\mu$. The statistical saturation bounds in the forced-dissipated case will be discussed in Section 5. In addition Figure 2.5 adds another large-scale forcing on first eigenmode $|\mathbf{k}| = 1$ with different strengths $\delta f$. This special case is also of its own interest and details will be discussed in Section 6.

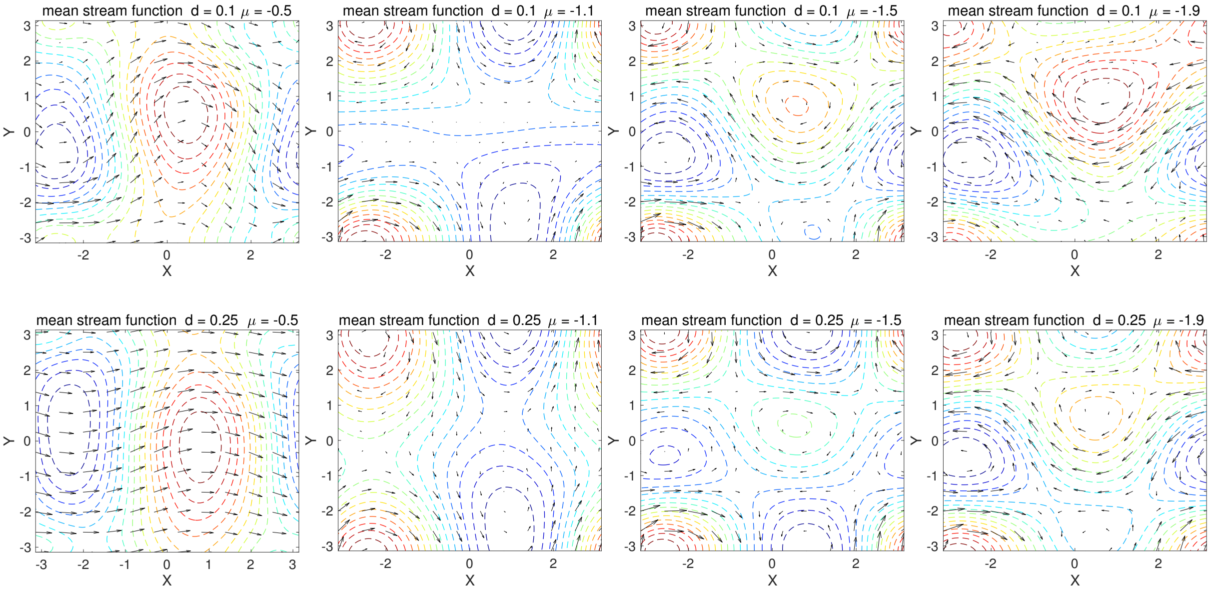


Fig. 2.4: Mean stream function in small scales (dashed contours) and the entire flow vector field including mean flow (vector field) are shown with different damping rates $d = 0.1, 0.25$ and parameter values $\mu = -0.5, -1.1, -1.5, -1.9$. The flow field shifts from eastward to blocked circulations to strong westward jet as the parameter $\mu$ changes.

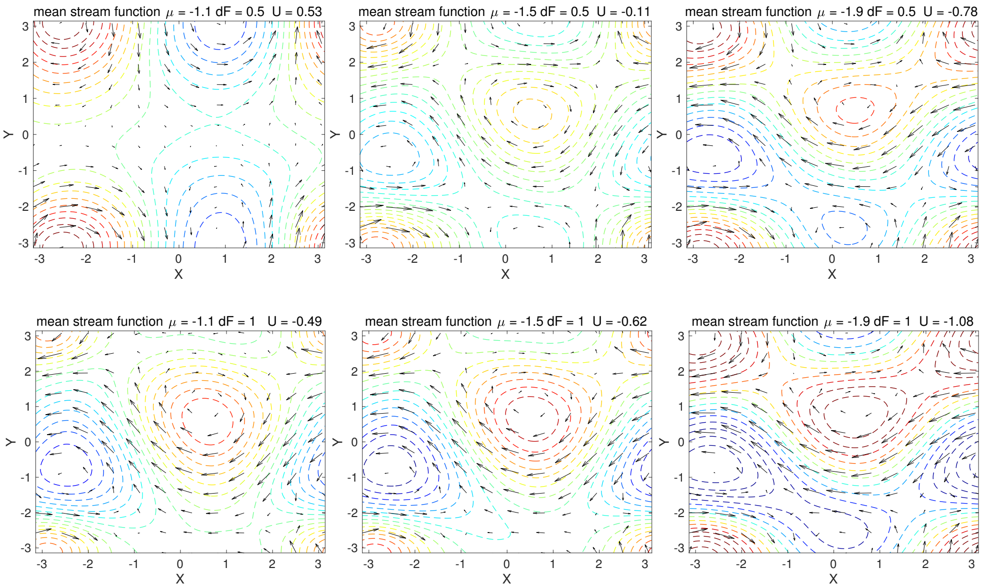


Fig. 2.5: Mean stream function in small scales (dashed contours) and the entire flow vector field including mean flow (vector field) with additional large-scale eigenmode forcing on the mean flow $U$ and the ground shell $|\mathbf{k}| = 1$ with strength $\delta F = 0.5, 1$. The steady state mean flow $\bar{U}$ is listed on the title.

## 3 Statistical Stability with Uncertainties from Initial Distributions in the Stable Regime

We first consider the statistical stability bounds of the barotropic flow due to the initial configuration of the ensemble distribution using the statistical energy equation for fluctuations. With the interaction of the large-scale flow and small-scale eddies, from the derivation before, we find the conserved statistical pseudo-energy in fluctuations (2.10)

$$E_{\mu}^{\mathrm{stat}}(t)=\frac{\mu}{2}\left\langle U^{2}\right\rangle_{t}+\frac{1}{2}\sum_{1\leq|\mathbf{k}|\leq\Lambda}\left(1+\mu\left|\mathbf{k}\right|^{-2}\right)\left\langle\left|\omega_{\mathbf{k}}\right|^{2}\right\rangle_{t}.$$

The subscript '$t$' refers to the ensemble average at time $t$. Remember that here $U$ represents the fluctuations from the steady state mean flow $V_{\mu}=-\beta/\mu$, and $\omega$ represents the fluctuations away from the steady state vorticity $Q_{\mu}$. Without external forcing and damping effects, the statistical pseudo-energy $E_{\mu}^{\mathrm{stat}}$ is conserved in time as shown in (2.11). Therefore the total statistical energy $E_{\mu}^{\mathrm{stat}}$ in the later time can be determined from the initial statistics in the mean fluctuation and variance, while the non-positive-definiteness of the total statistical energy forms another issue in the unstable regimes with negative coefficients. In this section, we first consider the simple case with $\mu>0$, so that the coefficients in each component of the total statistical energy are all positive.

### 3.1 Statistical energy bound in fluctuations without forcing and dissipation

We begin with the simple case in the stable regime $\mu>0$ and no damping and forcing terms on the right hand side of (2.7). Assume initial perturbations in the mean flow and eddies, $U(0)=\bar{U}_{0}+U_{0}^{\prime}$, $\omega(0)=\bar{\omega}_{0}+\omega_{0}^{\prime}$, where $\bar{U}_{0},\bar{\omega}_{0}$ are the initial bias in fluctuation mean states away from the steady state $V_{\mu},Q_{\mu}$, and $U_{0}^{\prime},\omega_{0}^{\prime}$ characterize the uncertainty (that is, ensemble variance) in the initial ensemble members. According to the steady state $(V_{\mu},Q_{\mu})$ with initial statistical energy in perturbation, the initial statistical energy can be expressed as

$$E_{\mu}^{\mathrm{stat}}(0)=\frac{\mu}{2}E_{U,0}+\frac{1}{2}\sum_{1\leq|\mathbf{k}|\leq\Lambda}\left(1+\mu\left|\mathbf{k}\right|^{-2}\right)E_{\mathbf{k},0},$$

with $E_{U,0}=\bar{U}_{0}^{2}+\overline{U_{0}^{\prime2}}$, and $E_{\mathbf{k},0}=\left|\bar{\omega}_{0,\mathbf{k}}\right|^{2}+\overline{|\omega_{0,\mathbf{k}}^{\prime}|^{2}}$. Especially we have the initial uncertainty from variance $\overline{|\omega_{0,\mathbf{k}}^{\prime}|^{2}}=\overline{|q_{0,\mathbf{k}}^{\prime}|^{2}}$ independent of the steady state, and the initial mean deviation for the fluctuation component with $\left|\bar{\omega}_{0,\mathbf{k}}\right|^{2}=\left|Q_{\mu,\mathbf{k}}-\bar{q}_{0,\mathbf{k}}\right|^{2}$ and $\bar{U}_{0}^{2}=\left|V_{\mu}-\bar{V}_{0}\right|^{2}$. Therefore due to the conservation of total statistical energy (2.11) we have the first statistical energy conservation relation

$$\sum_{1\leq|\mathbf{k}|\leq\Lambda}\mu_{\mathbf{k}}\left\langle\left|\omega_{\mathbf{k}}\right|^{2}\right\rangle_{t}+\mu\left\langle U^{2}\right\rangle_{t}\leq\sum_{1\leq|\mathbf{k}|\leq\Lambda}\mu_{\mathbf{k}}E_{\mathbf{k},0}+\mu E_{U,0},\tag{3.1}$$

with $\mu_{\mathbf{k}}=1+\mu\left|\mathbf{k}\right|^{-2}$ the weighting coefficients due to the energy conserving inner-product metric. In fact in (3.1) equality can be reached in the case without forcing and dissipation, while the inequality is valid for cases with also damping terms included in the system. Notice that the above relation is valid for all the values of $\mu$, whereas the statistics in the statistical fluctuations $\left\langle |\omega_{\mathbf{k}}|^2 \right\rangle$ (and in fact only in the statistical mean fluctuation part $|\bar{\omega}_{\mathbf{k}}|^2$) will change accordingly with different values of $\mu$ due to different values of the presumed mean state $Q_\mu$. We can summarize the first statistical energy bound for the stable regime $\mu > 0$ as follows:

**Theorem 1.** *(Statistical energy conservation of fluctuations in stable regime $\mu > 0$) Consider the system of fluctuation equations away from the steady state solution $(V_\mu, Q_\mu)$. For any parameter values $\mu > 0$ in the stable regime with $E_\mu > 0$, the total statistical variability in the mean fluctuation and variance, $\langle U^2 \rangle \equiv \bar{U}^2 + \overline{U'^2}$, $\langle |\omega_{\mathbf{k}}|^2 \rangle \equiv |\bar{\omega}_{\mathbf{k}}|^2 + \overline{|\omega'_{\mathbf{k}}|^2}$, can always be controlled by its initial statistical variability including initial mean and total variance as in the inequality (3.1). Especially, if there is no statistical mean perturbations in the initial time, $\bar{V}_0 = V_\mu$, $\bar{q}_0 = Q_\mu$, the total statistical energy of the system in the entire time can be controlled by the initial ensemble variances $\sigma^2_{\mathbf{k},0} = \overline{|\omega'_{0,\mathbf{k}}|^2}$ and $\sigma^2_{U,0} = \overline{U'^2}$*

$$\sum_{1\leq|\mathbf{k}|\leq\Lambda} \left(1+\mu\left|\mathbf{k}\right|^{-2}\right)\left\langle |\omega_{\mathbf{k}}|^2\right\rangle_t + \mu\left\langle U^2\right\rangle_t \leq \sum_{1\leq|\mathbf{k}|\leq\Lambda} \left(1+\mu\left|\mathbf{k}\right|^{-2}\right)\sigma^2_{\mathbf{k},0} + \mu\sigma^2_{U,0}. \tag{3.2}$$

*Furthermore, we can see both the statistical mean fluctuation and the variance are bounded by their initial variability in this stable regime with the inclusion of dissipation $d > 0$.*

Still the statistical bounds in (3.1) and (3.2) based on the pseudo-energy $E^{\text{stat}}_\mu$ directly is inconvenient to use since the coefficients on the left hand sides of the inequalities are dependent on the parameter values $\mu$. As a further implication of the above inequalities, we can find the statistical bounds for the total enstrophy, $⨍ \langle \omega^2 \rangle$, and the total kinetic energy, $U^2 + ⨍ \langle |\nabla\psi|^2 \rangle$. For the statistical enstrophy in the stable regime $\mu > 0$, there exists the lower bound among all the positive coefficients for any wavenumber $\mathbf{k}$ with truncation $\Lambda$

$$\left(1+\mu\left|\mathbf{k}\right|^{-2}\right)\left\langle |\omega_{\mathbf{k}}|^2\right\rangle \geq \left(1+\mu\Lambda^{-2}\right)\left\langle |\omega_{\mathbf{k}}|^2\right\rangle;$$

and for the statistical kinetic energy for any wavenumber $\mathbf{k}$ the lower bound of the coefficients becomes

$$\left(|\mathbf{k}|^2+\mu\right)\left\langle |\mathbf{k}|^2\left|\psi_{\mathbf{k}}\right|^2\right\rangle \geq \mu\left\langle |\mathbf{k}|^2\left|\psi_{\mathbf{k}}\right|^2\right\rangle.$$

Therefore the general bounds for the *total statistical enstrophy* $⨍ \langle \omega^2 \rangle \equiv \sum \langle |\omega_{\mathbf{k}}|^2 \rangle$ and the *total statistical kinetic energy* $\langle U^2 \rangle + ⨍ \langle |\nabla\psi|^2 \rangle \equiv \langle U^2 \rangle + \sum \langle |\mathbf{k}|^2 |\psi_{\mathbf{k}}|^2 \rangle$ can be determined by their initial conditions as

$$\begin{aligned}\sum_{1\leq|\mathbf{k}|\leq\Lambda}\left\langle |\omega_{\mathbf{k}}|^2\right\rangle_t &\leq \sum_{1\leq|\mathbf{k}|\leq\Lambda}\frac{1+\mu\left|\mathbf{k}\right|^{-2}}{1+\mu\Lambda^{-2}}E^q_{\mathbf{k},0} + \frac{\mu}{1+\mu\Lambda^{-2}}E^U_0,\\ \left\langle U^2\right\rangle_t + \sum_{1\leq|\mathbf{k}|\leq\Lambda}\left\langle |\mathbf{k}|^2\left|\psi_{\mathbf{k}}\right|^2\right\rangle_t &\leq \sum_{1\leq|\mathbf{k}|\leq\Lambda}\mu^{-1}\left(|\mathbf{k}|^2+\mu\right)|\mathbf{k}|^2 E^v_{\mathbf{k},0} + E^U_0,\end{aligned} \tag{3.3}$$

where the right hand sides are from the initial enstrophy/energy in the mean fluctuation and variance

$$E^q_{\mathbf{k},0} = \left|Q_{\mu,\mathbf{k}} - \bar{q}_{0,\mathbf{k}}\right|^2 + \overline{|q'_{0,\mathbf{k}}|^2},\ E^v_{\mathbf{k},0} = \left|\Psi_{\mu,\mathbf{k}} - \bar{\psi}_{0,\mathbf{k}}\right|^2 + \overline{|\psi'_{0,\mathbf{k}}|^2},\ E^U_0 = \left|V_\mu - \bar{U}_0\right|^2 + \overline{U'^2_0};$$

and on the left hand side the statistical enstrophy does not include the energy in the mean flow $U$ while it is still dependent on the initial configuration of the flow statistics $E_0^U$ due to the large-small scale interaction. The above bounds in (3.3) imply the stability in statistical mean and variance in each fluctuation mode under both the statistical enstrophy and kinetic energy metric in the stable regime with $\mu > 0$. Especially the variance $\overline{U'^2}, \overline{|\omega'_{\mathbf{k}}|^2}$, independent of the choices of the steady mean state $V_\mu, Q_\mu$, is one positive-definite component in the total statistical energy including mean and variance. The above statistical bounds illustrates that the total uncertainty in the ensemble variance (or it can be described as the 'spread' of the ensemble of trajectories) can always be controlled by the 'initial noises' from the initial ensemble uncertainty ($\overline{|q'_{0,\mathbf{k}}|^2}$ or $\overline{|\psi'_{0,\mathbf{k}}|^2}$) and the initial deviation in the statistical mean from the steady state solution $V_\mu, Q_{\mu,\mathbf{k}}$.

## 3.2 Numerical verification of the statistical bounds in the stable regime

Here we offer some simple numerical results to illustrate the statistical bounds in (3.2) and (3.3) in the stable regime $\mu > 0$. For simplicity, we assume there is no bias in the initial mean state, $\bar{V}_0 = V_\mu$, $\bar{q}_0 = Q_\mu$. And we propose two initial variance configurations in the ensembles. The first only gets non-zero initial variance only in the large scale mean flow $\sigma_U = 1$; and the second case assigns initial variance in the mean flow $U$ and first ground modes $|\mathbf{k}| = 1$, $\sigma_U = 1, \sigma_1 = 1$. The bounds in total statistical pseudo-energy (3.2) together with the statistical kinetic energy in (3.3) then can be simplified in the test cases as

$$\sum_{1\leq|\mathbf{k}|\leq\Lambda}\left(1+\mu\left|\mathbf{k}\right|^{-2}\right)\left\langle \left|\omega_{\mathbf{k}}\right|^{2}\right\rangle _{t}+\mu\left\langle U^{2}\right\rangle _{t}=4\left(1+\mu\right)\sigma_{1}^{2}+\mu\sigma_{U}^{2},\ \mu\sigma_{U}^{2};$$

$$\left\langle U^{2}\right\rangle _{t}+\sum_{1\leq|\mathbf{k}|\leq\Lambda}\left\langle \left|\mathbf{k}\right|^{2}\left|\psi_{\mathbf{k}}\right|^{2}\right\rangle _{t}\leq4\left(1+\mu\right)\sigma_{1}^{2}/\mu+\sigma_{U}^{2},\ \sigma_{U}^{2};$$

Above on the right hand sides, the first term is for the bounds with initial variance in $\sigma_U, \sigma_1$ and the second term is for the bounds with only initial variance in the mean flow $\sigma_U$. Notice that in the first relation above equality is actually reached since the total statistical energy is conserved in this case with no damping and forcing. Besides according to the equilibrium statistical mechanics, if the invariant measure (2.6) is reached at the final equilibrium with ergodicity [23] the above statistical estimates $\langle\cdot\rangle_t$ at equilibrium get zero mean in the fluctuation component and variances proportional to, $r_U \sim 1/\mu, r_{\mathbf{k}} \sim 1/\left(1+\mu\left|\mathbf{k}\right|^{-2}\right)$, according to the Gaussian invariant measure.

Figure 3.1 shows the results in the total statistical pseudo-energy and statistical kinetic energy with changing values of $\mu$. The statistical pseudo-energy conservation from numerical calculations is confirmed on the left panel exactly in agreement with the theoretical bounds from initial statistics with linear dependence on $\mu$. The bounds for the total statistical kinetic energy are also displayed with different initial conditions in right panel. The the steady flow structure and vorticity snapshot with parameter $\mu = 1$ have already been plotted in Figure 2.1 in Section 2.3. The kinetic energy bound from the pseudo-energy conservation in general can offer an accurate estimation about the maximum amplitude of statistical quantities as it changes with the steady state parameter $\mu$. We also compare the statistical mean and variance separately in the plots.

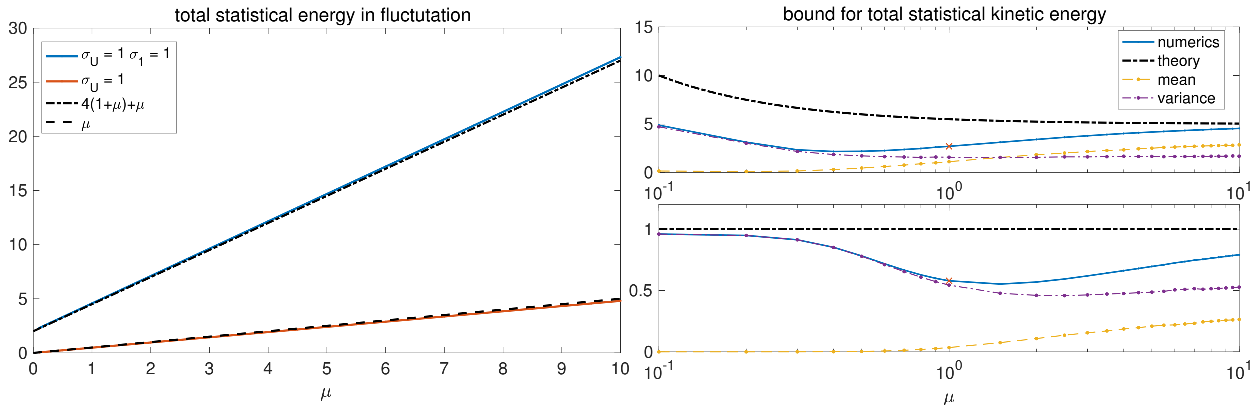


(a) total statistical pseudo-energy (b) statistical kinetic energy

Fig. 3.1: Statistical energy bounds in statistical equilibrium with $0 < \mu < 10$. The solid lines are the numerical simulation results and the dashed lines are from the theoretical bounds. In the right panel, the upper row is for the case with initial variance in $U, \omega_1$ and the lower row is the case with initial variance in $U$ only. Also the energy in the mean fluctuation and variance are compared separately. The value for the flow field shown in Figure 2.1 with $\mu = 1$ is marked with a red cross.

With smaller values of $\mu$, the invariant measure prediction in (2.6) is quite accurate. The fluctuation mean is near zero (thus the initial steady state solution $(V_\mu, Q_\mu)$ is maintained) and the variance in each mode is in consistent with the equilibrium measure prediction. As $\mu$ becomes larger, there gradually develops a non-zero mean fluctuation. This implies a new equilibrium steady state in the statistical mean, and correspondingly the variances in the system drop a little due to the transfer of energy to the mean state.

## 4 Statistical Saturation Bounds with Initial Uncertainties in Unstable Regimes

In the statistically stable regime $\mu > 0$ discussed above, the total statistical energy is positive-definite so the statistical bounds can be derived directly from the conservation of statistical energy. However in the statistically unstable regime with $\mu < 0$, the coefficients in the total statistical energy $E_\mu^{\text{stat}}$ in (2.10) are no longer uniformly positive. In this case, between two adjacent wave numbers $-\Lambda_{\mu+1}^2 < \mu < -\Lambda_\mu^2$ (in this notation, $\Lambda_\mu^2$ and $\Lambda_{\mu+1}^2$ are two adjacent integer energy shells, while $\Lambda_\mu, \Lambda_{\mu+1}$ could be non-integers)

$$\begin{aligned} 1 + \mu \left|\mathbf{k}\right|^{-2} > 0, &\quad \left|\mathbf{k}\right| \geq \Lambda_{\mu+1}, \\ 1 + \mu \left|\mathbf{k}\right|^{-2} < 0, &\quad \left|\mathbf{k}\right| \leq \Lambda_\mu. \end{aligned} \tag{4.1}$$

Therefore, the total statistical energy $E_\mu^{\text{stat}}$ needs to be decomposed into two parts with a positive-definite component and a negative-definite component

$$\begin{aligned} E_\mu^{\text{stat}} &= -E_\mu^L + E_\mu^S \\ E_\mu^L &= \frac{1}{2} \sum_{1 \leq |\mathbf{k}| \leq \Lambda_\mu} \left|1 + \mu \left|\mathbf{k}\right|^{-2}\right| \left\langle \left|\omega_\mathbf{k}\right|^2 \right\rangle + \frac{|\mu|}{2} \left\langle U^2 \right\rangle, \\ E_\mu^S &= \frac{1}{2} \sum_{|\mathbf{k}| \geq \Lambda_{\mu+1}} \left(1 + \mu \left|\mathbf{k}\right|^{-2}\right) \left\langle \left|\omega_\mathbf{k}\right|^2 \right\rangle. \end{aligned} \tag{4.2}$$

Above in (4.2) $E_{\mu}^{L}$ is the large scale statistical energy with negative coefficients, and $E_{\mu}^{S}$ is the rest statistical energy in small scales with positive coefficients. Especially in regime $-1<\mu<0$, only the large scale mean flow $U$ is contained in $E_{\mu}^{L}$. This is an interesting case where the interactions between the large mean flow $U$ and small vortical modes $\omega$ become important through topographic stress.

In general, $E_{\mu}^{S}$ will contain many more modes with high wavenumbers and $E_{\mu}^{L}$ usually only gets the modes in the largest scales (which also usually are of more interest). This implies the possible instability between the low wavenumber and high wavenumber modes in this regime. Still without the external damping and noise terms the total statistical energy conservation from (2.11) is valid,

$$E_{\mu}^{\mathrm{stat}}\left(t\right)=E_{\mu}^{\mathrm{stat}}\left(0\right).$$

Suppose negative initial statistical energy $E_0=E_{\mu,0}^{S}-E_{\mu,0}^{L}<0$, that is, at initial time $t=0$

$$\sum_{|\mathbf{k}|\geq\Lambda_{\mu+1}}\left(1+\mu\left|\mathbf{k}\right|^{-2}\right)\left\langle\left|\omega_{\mathbf{k}}\right|^{2}\right\rangle_{0}\leq\sum_{|\mathbf{k}|\leq\Lambda_{\mu}}\left|1+\mu\left|\mathbf{k}\right|^{-2}\right|\left\langle\left|\omega_{\mathbf{k}}\right|^{2}\right\rangle_{0}+\left|\mu\right|\left\langle U^{2}\right\rangle_{0}. \tag{4.3}$$

This implies larger initial perturbations (both in mean and noise) in the unstable larger scales, and this should be a natural case that is easy to satisfy in many realistic scenarios [17,22]. As a result, the conservation law of the total statistical energy in fluctuation predicts that the perturbed mean and variance in all the high wavenumber modes are 'slaved' by the low wavenumber large-scale perturbations in mean and variance during all the time

$$\sum_{|\mathbf{k}|\geq\Lambda_{\mu+1}}\left(1+\mu\left|\mathbf{k}\right|^{-2}\right)\left\langle\left|\omega_{\mathbf{k}}\right|^{2}\right\rangle_{t}\leq\sum_{|\mathbf{k}|\leq\Lambda_{\mu}}\left|1+\mu\left|\mathbf{k}\right|^{-2}\right|\left\langle\left|\omega_{\mathbf{k}}\right|^{2}\right\rangle_{t}+\left|\mu\right|\left\langle U^{2}\right\rangle_{t}. \tag{4.4}$$

Still this inequality cannot guarantee the general statistical stability in the total energy in mean and variance since both sides of (4.4) could grow (or decay) without bound at the same time [17]. In the remainder of this section, we consider the saturation bounds of the total statistical mean and variance specially in the unstable regime $\mu<0$ using the similar idea for deterministic saturation bounds in [29]. No external forcing and dissipation is assumed here so that the problem is to determine how the statistics in the system evolve in time according to the steady state solution $(V_\mu,Q_\mu)$ from the initial ensemble distribution.

### 4.1 Statistical energy saturation bounds without forcing and dissipation

In deriving the statistical bounds in the unstable regimes, we make use of the positive-definite conserved statistical functional in Section 3 to find the saturation of instability in the topographic barotropic flow. In order to apply the previous result, we propose a class of statistically stable 'reference states' with parameters $\alpha>0$. Thus about the reference steady state (2.4) in the potential vorticity, stream function, and large scale mean flow

$$Q_{\alpha,\mathbf{k}}=\frac{\alpha\hat{h}_{\mathbf{k}}}{\alpha+\left|\mathbf{k}\right|^{2}},\quad\Psi_{\alpha,\mathbf{k}}=\frac{\hat{h}_{\mathbf{k}}}{\alpha+\left|\mathbf{k}\right|^{2}},\quad V_{\alpha}=-\frac{\beta}{\alpha},$$

the total statistical energy in fluctuation (2.10) about the reference state stays conserved depending on the initial state statistics, that is,

$$E_{\alpha}^{\mathrm{stat}}\left(t\right)=\frac{\alpha}{2}\left\langle \left(U-V_{\alpha}\right)^{2}\right\rangle_{t}+\frac{1}{2}\sum_{1\leq\left|\mathbf{k}\right|\leq\Lambda}\left(1+\alpha\left|\mathbf{k}\right|^{-2}\right)\left\langle \left|q_{\mathbf{k}}-Q_{\alpha,\mathbf{k}}\right|^{2}\right\rangle_{t}\equiv E_{\alpha}^{\mathrm{stat}}\left(0\right). \tag{4.5}$$

Therefore the previous statistical bound in (3.1) is still valid according to the reference state for all $\alpha>0$. In this way the coefficients in each component of the total statistical energy $E_{\alpha}^{\mathrm{stat}}$ again become uniformly positive. Now we turn to the steady state solutions in the unstable regime $\mu<0$ so that we get two sets of decompositions with the real steady state with $\mu$ and the reference state with $\alpha$

$$U\left(t\right)=V_{\mu}+\tilde{U}\left(t\right)=V_{\alpha}+\hat{U}\left(t\right),\quad q\left(t\right)=Q_{\mu}+\tilde{\omega}\left(t\right)=Q_{\alpha}+\hat{\omega}\left(t\right).$$

Thus we can rewrite the statistics in the fluctuation components $\left(\tilde{U},\tilde{\omega}\right)$ about the steady state solution $\left(V_{\mu},Q_{\mu}\right)$ according to the previous stable reference state with parameter $\alpha$ as

$$\begin{aligned}\left\langle \left(U-V_{\alpha}\right)^{2}\right\rangle &=\left(V_{\mu}-V_{\alpha}+\bar{U}\right)^{2}+\overline{U'^{2}},\\ \left\langle \left|q_{\mathbf{k}}-Q_{\alpha,\mathbf{k}}\right|^{2}\right\rangle &=\left|Q_{\mu,\mathbf{k}}-Q_{\alpha,\mathbf{k}}+\bar{\omega}_{\mathbf{k}}\right|^{2}+\overline{\left|\omega_{\mathbf{k}}'\right|^{2}},\end{aligned}$$

where we can define the constants between the steady state and the reference state as

$$V_{\mu,\alpha}\equiv V_{\mu}-V_{\alpha}=\frac{\alpha-\mu}{\alpha}V_{\mu},\quad Q_{\mu,\alpha,\mathbf{k}}\equiv Q_{\mu,\mathbf{k}}-Q_{\alpha,\mathbf{k}}=\frac{\left(\mu-\alpha\right)\left|\mathbf{k}\right|^{2}}{\alpha+\left|\mathbf{k}\right|^{2}}\Psi_{\mu,\mathbf{k}}. \tag{4.6}$$

Then we get the statistical energy bound for the fluctuation component $\left(\tilde{U},\tilde{\omega}\right)$ based on the conservation of the positive-definite total statistical energy $E_{\alpha}^{\mathrm{stat}}\left(t\right)=E_{\alpha}^{\mathrm{stat}}\left(0\right)$ according to the reference state with parameter $\alpha>0$. The initial statistical energy can be calculated as in (4.5) with the initial mean fluctuation $\left(\bar{U}_{0},\bar{\omega}_{0}\right)$ and the initial variance $\left(\overline{U_{0}'^{2}},\overline{\left|\omega_{0}'\right|^{2}}\right)$ in large scale mean flow and small vortical modes. The previous argument is based on the fact that the topographic barotropic system without forcing and dissipation always conserves the total statistical energy for any values of the parameter $\alpha$, thus we have the additional freedom to choose the optimal parameter value $\alpha$ in the conservation relation (4.5) for the saturation of statistical instability in the unstable regime.

The goal here is to find the statistical bound of fluctuations about the steady state solution $\left(V_{\mu},Q_{\mu}\right)$ in the unstable regime $\mu<0$. Again we propose the initial state with zero perturbation in statistical mean about the steady state solution and prescribed variances in each mode

$$\bar{U}_{0}=0,\ \bar{\omega}_{0}=0,\quad \overline{U_{0}'^{2}}=\sigma_{U,0}^{2},\ \overline{\left|\omega_{\mathbf{k},0}'\right|^{2}}=\sigma_{\mathbf{k},0}^{2}. \tag{4.7}$$

Without the inclusion of external forcing and dissipation, the problem is to track the evolution and amplification of the fluctuations in the ensemble of particles beginning with an unbiased initial steady state and proper amount of uncertainty among the ensemble of particles. Then by applying the conservation of total statistical energy (4.5) the mean fluctuation and variance can be determined by the initial configuration of variance and the difference with the reference state

$$\begin{aligned} & \alpha\left[\left(V_{\mu,\alpha}+\bar{U}_t\right)^2+\overline{U_t'^2}\right]+\sum_{1\leq|\mathbf{k}|\leq\Lambda}\left(1+\alpha\left|\mathbf{k}\right|^{-2}\right)\left[\left|Q_{\mu,\alpha,\mathbf{k}}+\bar{\omega}_{\mathbf{k},t}\right|^2+\overline{|\omega_{\mathbf{k},t}'|^2}\right] \\ = & \quad \alpha\left[V_{\mu,\alpha}^2+\sigma_{U,0}^2\right]+\sum_{1\leq|\mathbf{k}|\leq\Lambda}\left(1+\alpha\left|\mathbf{k}\right|^{-2}\right)\left[\left|Q_{\mu,\alpha,\mathbf{k}}\right|^2+\sigma_{\mathbf{k},0}^2\right]. \end{aligned} \tag{4.8}$$

The above equality is valid for all the values of $\alpha>0$. Instead of the slaving relation (4.4) that separates the whole system into a stable and an unstable subspace with $\mu<0$, the relation in (4.8) gets uniformly positive coefficients in every component of the statistical energy in the mean fluctuation and variance. The evolution of the combined statistics in mean and variance in the future time are determined purely by the initial statistical configuration in mean difference $(V_{\mu,\alpha},Q_{\mu,\alpha,\mathbf{k}})$ and ensemble spread $(\sigma_{U,0},\sigma_{\mathbf{k},0})$. Therefore immediately we get the statistical stability in each component of the fluctuation mean and variance that they will stay finite and stable as the system evolves in time since the right hand side in the initial value is finite with positive coefficients. That is, when we run an ensemble with initial steady state $(V_\mu,Q_\mu)$ with statistical uncertainties in particles, the bias in the mean state and the spread of the ensemble will always stay finite in amplitude without unbounded growth. On the other hand, still the conservation relation in (4.8) is not convenient in calculating the statistical bounds since it is combined with the difference in the reference state $V_{\mu,\alpha}$ and $Q_{\mu,\alpha}$ and the reference parameter $\alpha$. Next we try to find the saturation bound for the statistics in fluctuation mean and variance by minimizing the right hand side among all the values of $\alpha>0$. Especially we consider the saturation bounds for the total statistical kinetic energy in the mean, $\bar{U}^2+\fint|\nabla\bar{\psi}|^2$, and in the variance, $\overline{U'^2}+\fint\overline{|\nabla\psi'|^2}$ as a representative example. In a similar way the saturation bounds for enstrophy can also be achieved (see Section 6 for an example of the statistical enstrophy bound).

*Saturation bound for total variance based on the kinetic energy*

In the first place we can look at the saturation bound for the second order moments. To consider the variance in the kinetic energy from the conservation relation (4.8), we can just leave the leading order parts involving the mean states with positive coefficients in the total statistical energy. Then for all values $\alpha>0$ we have

$$\overline{U_t'^2}+\sum\left|\mathbf{k}\right|^2\overline{\left|\psi_{\mathbf{k},t}'\right|^2}\leq\left[\left(V_{\mu,\alpha}+\bar{U}_t\right)^2+\overline{U_t'^2}\right]+\sum\left(\alpha^{-1}\left|\mathbf{k}\right|^2+1\right)\left|\mathbf{k}\right|^2\left[\left|\Psi_{\mu,\alpha,\mathbf{k}}+\bar{\psi}_{\mathbf{k},t}\right|^2+\overline{\left|\psi_{\mathbf{k},t}'\right|^2}\right], \tag{4.9}$$

where the left hand side above defines the *total statistical kinetic energy* in the variance, $\overline{U'^2}+\fint\overline{|\nabla\psi'|^2}$, and the right hand side is just a reorganization of the total statistical pseudo-energy $\alpha^{-1}E_\alpha$ writing in the form of stream functions, $\psi_{\mathbf{k}}=-\left|\mathbf{k}\right|^{-2}\omega_{\mathbf{k}}$. Using the conservation relation in (4.8) to relate the right hand side of the above inequality with the initial data and noting that the above inequality is valid for all values $\alpha>0$, the saturation bound for the total statistical kinetic energy variance (4.9) can be reached by minimizing the second row of (4.8) including initial state information among all the possible values of $\alpha$ so that we define

$$C_{\mu}^{v}=\min_{\alpha>0}\left[\frac{(\alpha-\mu)^{2}}{\alpha^{2}}V_{\mu}^{2}+\sigma_{U,0}^{2}\right]+\sum_{1\leq|\mathbf{k}|\leq\Lambda}\left[\frac{(\alpha-\mu)^{2}\,|\mathbf{k}|^{2}}{\alpha\left(\alpha+|\mathbf{k}|^{2}\right)}\left|\Psi_{\mu,\mathbf{k}}\right|^{2}+\left(|\mathbf{k}|^{-2}+\alpha^{-1}\right)\sigma_{\mathbf{k},0}^{2}\right],$$

with $V_{\mu}=-\beta/\mu$ and $\Psi_{\mu,\mathbf{k}}=\hat{h}_{\mathbf{k}}/\left(\mu+|\mathbf{k}|^{2}\right)$ the steady state solutions and the initial ensemble statistics based on (4.7). The differences with reference states $V_{\mu,\alpha},Q_{\mu,\alpha}$ in (4.6) are substituted into the initial values in the second row of (4.8) to get an explicit formulation of the upper bound. The total variance of the flow fluctuation in both large scale mean flow and small vorticity thus are controlled by the saturation bound

$$\overline{U_{t}^{\prime 2}}+\sum_{1\leq|\mathbf{k}|\leq\Lambda}|\mathbf{k}|^{2}\,\overline{\left|\psi_{\mathbf{k},t}^{\prime}\right|^{2}}\leq C_{\mu}^{v}\left(h,\beta,\sigma_{0},\Lambda\right),\tag{4.10}$$

where the bound $C_{\mu}^{v}$ is dependent on the truncation size $\Lambda$, topographic structure $h$, the beta-effect $\beta$, and the initial noise in each mode $\sigma_0$. The saturation bound $C_{\mu}^{v}$ estimates the maximum amount of energy in variance the system could reach depending on the initial statistical configuration. Indeed more generally $C_{\mu}^{v}$ also gives the upper bound for the right hand side of (4.9) directly from the conservation principle in (4.8). Especially as we will see later, the bound in variance $C_{\mu}^{v}$ is also useful in estimating a (non-optimal) upper bound for the statistical energy in the mean fluctuation, and it is also adapted to estimate a bound for a combination of the mean and variance together. Thus the saturation bound $C_{\mu}^{v}$ plays a central role in estimating the flow statistical instability.

*Remark.* Here we choose the statistical kinetic energy as the quantity of interest for the saturation bound since it offers a natural combination of large scale mean flow $U$ and vortical modes $\omega$ to characterize the total statistical structure in the system. In a similar fashion we can also get the estimation for the total statistical enstrophy based on the conservation relation (see Section 6 for one example with statistical enstrophy). Indeed since each component in the first row of (4.8) is positive definite, we can even find the saturation bound for any particular spectral band containing a fraction of the total wavenumbers. Therefore the relation in (4.8) is a quite useful tool to find the saturation bounds according to the required quantity of interest in real applications.

In Figure 4.1, we plot the saturation bounds $C_{\mu}^{v}$ with changing values of $\mu$ for the statistical kinetic energy by minimization among values in the stable regime $\alpha>0$. The model parameters are kept the same with the previous setup in Section 2.3 with $\beta=1$, $\Lambda=12$, and $h$ the topography with decaying spectrum in (2.14). In the figure we use non-zero topography up to wavenumber $|\mathbf{k}|=5$ as an illustration. Initial variance is only set to be non-zero among the mean flow $\sigma_{U,0}=1$ and the ground modes $|\mathbf{k}|=1$ with variance $\sigma_{1,0}=1$. The saturation bound $C_{\mu}^{v}$ goes to infinity at the discrete resonance points at $\mu=-|\mathbf{k}|^{2}$ with non-zero 'excited' topographic mode $\hat{h}_{\mathbf{k}}\neq0$, and stays in finite constraint values between the points. For values of $\mu$ near these saturation points, the large values of the bound $C_{\mu}^{v}$ indicate instability with potential large increase in the total variances in the fluctuation component from the initial uncertainty. On the other hand for values away from the resonance points the total statistical variance can be controlled

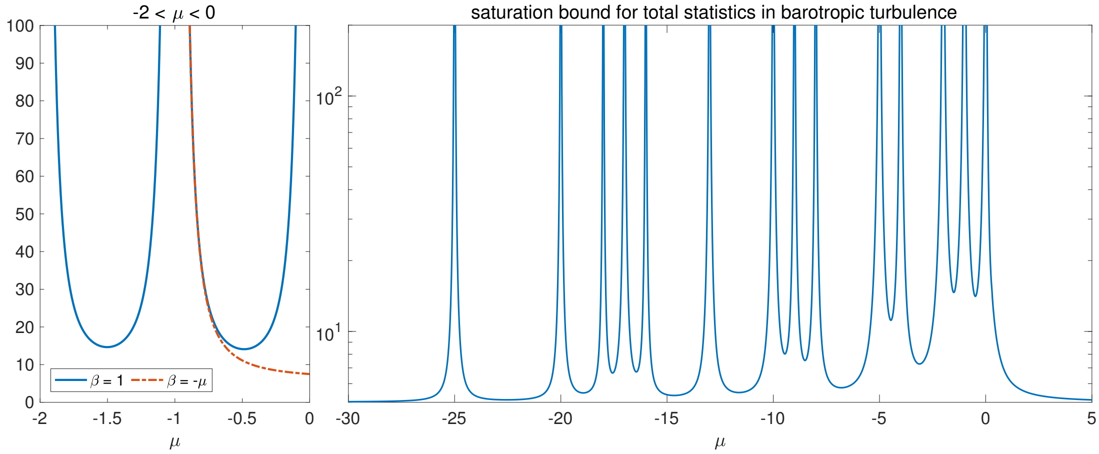


Fig. 4.1: Saturation bound $C_\mu^v$ for the total variance in kinetic energy (4.10). Initial variance is only set to be non-zero among the mean flow $\sigma_{U,0} = 1$ and the ground modes $|\mathbf{k}| = 1$ with variance $\sigma_{1,0} = 1$. The left panel shows the bounds in regimes $-2 < \mu < 0$ used for numerical verifications.

within relatively small values, implying restricted variability in the statistical ensemble with stability. In the numerical verification for the statistical bound, we will mostly focus on two typical regimes with parameters changing among the ranges $-2 < \mu < -1$ and $-1 < \mu < 0$ shown in the left panel of Figure 4.1. We point out here in advance that the total statistical energy in fluctuation near $\mu \to 0$ actually will not increase in reality since there is actually no instability near this point (see Appendix A with transient statistical stability). Therefore instead in the regime $-1 < \mu < 0$ we choose the $\beta$-effect in the constant ratio $\beta/\mu = -1$, so that stronger variability in the state variables can be generated near the limit $\mu \to 0$.

*Saturation bound for total statistical fluctuations in a combination of energy in the mean and variance*

The above saturation bound about the total variance (4.10) could be tight if the deviation in the statistical mean $|Q_{\mu,\alpha,\mathbf{k}} + \bar{\omega}_{\mathbf{k}}|$ is small (for example, when there is only weak topographic stress in small amplitude, $h \sim 0$). Still the error due to the previous neglected statistical mean from the term $Q_{\mu,\alpha}$ needs to be addressed, and it is difficult to estimate the energy in the statistical mean fluctuation $\bar{\omega}$ directly from the previous inequalities. Especially when there are some values of $|\mathbf{k}|^2$ close to $-\mu$, the errors from $Q_{\mu,\alpha}$ could be huge (due to the singularity in $Q_{\mu,\mathbf{k}}$). There is the possibility that large amount of energy could cascade from the variances back to the statistical mean state due to the nonlinear interactions and drive the mean state $\bar{\omega}$ away to another distinct state as the system evolves in time. Next we find a more general saturation bound for the combined fluctuation statistical mean and variance through proper estimation about the error in the mean.

In general we have the inequality to separate the statistical mean fluctuation and the additional difference term $Q_{\mu,\alpha}$ as

$$\begin{aligned}\left|Q_{\mu,\alpha,\mathbf{k}} + \bar{\omega}_{\mathbf{k}}\right|^2 &= \left|Q_{\mu,\alpha,\mathbf{k}}\right|^2 + \left|\bar{\omega}_{\mathbf{k}}\right|^2 - 2\mathfrak{Re}\left(Q_{\mu,\alpha,\mathbf{k}} \cdot \bar{\omega}_{\mathbf{k}}^*\right) \\ &\geq \left(1 - \epsilon^{-1}\right)\left|Q_{\mu,\alpha,\mathbf{k}}\right|^2 + (1-\epsilon)\left|\bar{\omega}_{\mathbf{k}}\right|^2,\end{aligned}$$

where Cauchy's inequality is used for the cross term, $Q_{\mu,\alpha,\mathbf{k}}\cdot\bar{\omega}_{\mathbf{k}}^{*}$, with $\epsilon>0$ as a control parameter. Similarly for the large scale flow $U$ we have the inequality to separate the mean fluctuation and the difference term $V_{\mu,\alpha}$ as

$$\left(V_{\mu,\alpha}+\bar{U}\right)^{2}\geq\left(1-\epsilon^{-1}\right)V_{\mu,\alpha}^{2}+\left(1-\epsilon\right)\bar{U}^{2}.$$

Substituting the above inequalities for each mode back into the total statistical energy conservation relation (4.8), we have the bound for total statistical energy depending on the initial value

$$\begin{aligned}&\left[\left(1-\epsilon\right)\bar{U}_{t}^{2}+\overline{U_{t}^{\prime2}}\right]+\sum\left(\alpha^{-1}\left|\mathbf{k}\right|^{2}+1\right)\left[\left(1-\epsilon\right)\left|\mathbf{k}\right|^{2}\left|\bar{\psi}_{\mathbf{k},t}\right|^{2}+\left|\mathbf{k}\right|^{2}\overline{\left|\psi_{\mathbf{k},t}^{\prime}\right|^{2}}\right]\\ \leq\;&\left[\epsilon^{-1}V_{\mu,\alpha}^{2}+\sigma_{U,0}^{2}\right]+\sum\left(\alpha^{-1}+\left|\mathbf{k}\right|^{-2}\right)\left[\epsilon^{-1}\left|Q_{\mu,\alpha,\mathbf{k}}\right|^{2}+\sigma_{\mathbf{k},0}^{2}\right].\end{aligned}\tag{4.11}$$

In the first row above we use the statistical kinetic energy representation as in (4.9). Still we assume that initial statistical mean of the ensemble has no bias in the steady state mean $(V_\mu, Q_\mu)$ and the initial ensemble variance has spectrum for mean flow and small scale modes $\overline{U_0^{\prime2}}=\sigma_{U,0}^2, \overline{|\omega_{\mathbf{k},0}^{\prime}|^2}=\sigma_{\mathbf{k},0}^2$ as before. Fortunately the difference terms $|Q_{\mu,\alpha,\mathbf{k}}|^2$ and $V_{\mu,\alpha}^2$ appear on both sides of the above inequality and get cancelled with each other. The inequality is valid for all the values with $\epsilon>0,\alpha>0$. Then we get the bounds for combinations of statistical mean fluctuation and the variance with a ratio $1-\epsilon$. Especially if we take $\epsilon=1$ only the statistical energy in variance is left and we come back to the original case (4.10). However $\epsilon$ can not reach the value zero (then the right hand side will diverge). Thus instead of a total statistical energy combining the mean and variance as $E^m+E^v$, the saturation bound can only be reached for the combination $\theta E^m+E^v$ with a weighting parameter $\theta=1-\epsilon^{-1}<1$. To get the total statistical kinetic energy, further reduce the coefficients in the above inequality (4.11), $\alpha^{-1}\left|\mathbf{k}\right|^2+1\geq1$, to a uniform lower bound. We find the general saturation bound combining the statistical mean fluctuation and variance as

$$C_{\mu}^{\theta}=\min_{\alpha>0}\frac{1}{1-\theta}\left[\frac{\left(\alpha-\mu\right)^{2}}{\alpha^{2}}V_{\mu}^{2}+\sum\frac{\left(\alpha-\mu\right)^{2}\left|\mathbf{k}\right|^{2}}{\alpha\left(\alpha+\left|\mathbf{k}\right|^{2}\right)}\left|\Psi_{\mu,\mathbf{k}}\right|^{2}\right]+\left[\sigma_{U,0}^{2}+\sum\left(\left|\mathbf{k}\right|^{-2}+\alpha^{-1}\right)\sigma_{\mathbf{k},0}^{2}\right].$$

The combined statistical energy in the mean fluctuation and variance with a weighting parameter $\theta<1$ can be estimated by this total saturation bound

$$\theta E^{m}\left(t\right)+E^{v}\left(t\right)\leq C_{\mu}^{\theta}\left(h,\beta,\sigma_{0},\Lambda\right),\tag{4.12}$$

where $E^m$ is the statistical energy in the mean fluctuation and $E^v$ is the statistical variance

$$\begin{aligned}E^{m}&=\bar{U}^{2}+\fint\left|\nabla\bar{\psi}\right|^{2}=\bar{U}^{2}+\sum\left|\mathbf{k}\right|^{2}\left|\bar{\psi}_{\mathbf{k}}\right|^{2},\\ E^{v}&=\overline{U^{\prime2}}+\fint\overline{\left|\nabla\psi^{\prime}\right|^{2}}=\overline{U^{\prime2}}+\sum\left|\mathbf{k}\right|^{2}\overline{\left|\psi_{\mathbf{k}}^{\prime}\right|^{2}}.\end{aligned}$$

Comparing (4.12) with (4.10), $C_\mu^\theta$ differs with $C_\mu^v$ only with one additional coefficient $(1-\theta)^{-1}$ and it reduces to the variance bound $C_\mu^v$ when the parameter $\theta\to0$ with consistency. Unfortunately we cannot reach the total statistical energy bound for $\theta=1$ in the above saturation bound $C_\mu^\theta$. Notice that in (4.12) we can even have $\theta < 0$, then the inequality describes that the total variance in second order moments in the system can actually be controlled by the total energy in the first order mean state.

Further a non-optimal bound for the statistical mean state purely can be found through further approximation in the combined statistical energy. By leaving the variance part in the inequality, $\theta E^m \leq \theta E^m + E^v \leq C_\mu^\theta$, from the above total statistical bound (4.12), then the energy in the mean fluctuation $E^m$ can be estimated by the previous total variance bound so that

$$\bar{U}_t^2 + \sum_{1 \leq |\mathbf{k}| \leq \Lambda} |\mathbf{k}|^2 \left|\bar{\psi}_{\mathbf{k},t}\right|^2 \leq C_\mu^m = \min_{\theta < 1} \theta^{-1} (1-\theta)^{-1} C_\mu^v = 4C_\mu^v. \tag{4.13}$$

The above inequality is through a crude approximation by leaving the total variance $E^v$ on the left side of (4.12) entirely, thus could introduce large errors in the bound of total mean fluctuation $E^m$. Nevertheless $C_\mu^m$ offers an estimation for the deviation in statistical mean from the original steady state solution instead of including the errors in the variances.

In the above argument we offer three levels of estimations. The first inequality in (4.11) actually offers a most general bound directly from the conservation of total statistical pseudo-energy including the coefficients $1 + \alpha |\mathbf{k}|^{-2}$. Through this relation we can derive the saturation bound based on any specific quantity of interest in practical applications. The next inequality (4.12) considers a proper combination of the total statistical mean fluctuation and total variance with a balance parameter $\theta$ according to the kinetic energy. This saturation bound $C_\mu^\theta$ is a general result for total statistical kinetic energy including both information in the mean and variance. The pure saturation bound for total variance $C_\mu^v$ in (4.10) can be derived from $C_\mu^\theta$ by setting $\theta = 0$. However notice that larger value of $\theta$ near 1 (then more emphasis on the stability in statistical mean) leads to a larger weight $1/(1-\theta)$ in the bound $C_\mu^\theta$. This shows that $C_\mu^\theta$ may not be so desirable if we want to add more emphasis on the mean fluctuation. In the last inequality (4.13), we separate the statistical mean state. It shows that the total statistical mean fluctuation also can not increase without bound with a largest amplitude $C_\mu^m = 4C_\mu^v$, while this bound is not optimal since $C_\mu^v$ could become huge.

**Theorem 2.** *(Statistical saturation bound for total statistical mean fluctuation and variance) For any general values of $\mu$ (and especially for the unstable case $\mu < 0$) in the topographic barotropic system without forcing and dissipation, assume zero initial statistical mean fluctuation and a general initial ensemble variance as (4.7). A saturation bound for a combination of the statistical mean and variance, $\theta E^m + E^v$, with a ratio parameter $\theta \in (0, 1)$ can be reached from (4.12). Especially the total variance in the kinetic energy, $E^v$, can be controlled with a saturation bound $C_\mu^v$ from (4.10); and for the total statistical energy in the mean fluctuation only, a (non-optimal) estimation of the saturation bound $C_\mu^m = 4C_\mu^v$ can be found as (4.13).*

### 4.2 Numerical verification of the saturation bounds in unstable regimes

In the final part of this section, we verify these saturation bounds for both the variance and the mean state through numerical simulations. The model parameters for the numerical simulations are taken the same as in Section 2.3. We test two typical regimes for the parameter $-2<\mu<-1$ and $-1<\mu<0$ with the saturation bounds shown in Figure 4.1. The complexity of the flow structures in these test regimes with strong instability and shifting directions of jets has already been illustrated in Figure 2.3 and Table 1. Instead of comparing the statistical energy in mean and variance separately, here we consider the saturation bound $C_{\mu}^{\theta}$ for the combination of mean fluctuation and variance $\theta E^{m}\left(t\right)+E^{v}\left(t\right)$ with changing values of $\theta$.

### *4.2.1 Saturation bound in the unstable regime $\mu<-1$*

First we check the saturation bound for total variance and mean in the unstable regime with parameter values changing among $-2<\mu<-1$. The flow field structures in this regime can be found in Figure 2.3 for typical values $\mu=-1.9,-1.5,-1.1$. Figure 4.2 illustrates the bounds of a combined mean fluctuation and variance with the parameter $\theta$ from the inequality (4.12). $\theta$ sets the weight in the statistical mean state. We check two parameter values $\theta=0.5$ and $\theta=0.2$. With $\theta=0.5$ the mean fluctuation part makes more contribution in the total statistical energy, while with $\theta=0.2$ the statistical energy in the variance is dominant. First the dotted-dashed black lines illustrate the theoretical saturation bounds $C_{\mu}^{\theta}$ with changing values of $\mu$. As expected from the theoretical results, instability with infinite maximum total statistics will take place at the resonance points $\mu=-1,-2$. From the numerical results, the saturation bound $C_{\mu}^{\theta}$ sets a tight upper bound in general and instability increases when $\mu$ approaches near the two end points in both cases. Especially in the case with $\theta=0.2$ where the variance part is dominant, from the expanded plot in results near $\mu\rightarrow-2$ the saturation bound becomes extremely tight for the combined statistics. This shows the accuracy in the upper bound $C_{\mu}^{\theta}$ for estimating the maximum statistical fluctuations in this highly unstable regime. With larger weight in the mean fluctuation, the larger value of $\theta=0.5$ raises the saturation bound $C_{\mu}^{\theta}$ as shown in (4.12). Still an accurate upper bound can be achieved especially for quantifying the variability in the statistical mean state. For the intermediate values of $\mu$ the maximum statistical energy is relatively low and the saturation bound still serves as a proper estimation for the maximum statistical energy in mean and variance. Furthermore, we can observe that the instability increases faster near the left side boundary than that near the right side. This might be related with the stronger linear instability in the left limit (see the Appendix A).

### *4.2.2 Saturation bound in the regime with unstable mean flow $-1<\mu<0$*

In the second case, we check the saturation bound in regime $-1<\mu<0$ with only an unstable mean flow $U$. We use smaller beta-effect $\beta=|\mu|$ to reduce the stabilizing effect from $\beta$ as the parameter approaches zero $\mu\rightarrow0$. This is considering the weaker variability in the flow fluctuation as $\mu$ decreases (as we can see from the linear analysis in Appendix A, when $\mu$ approaches zero with a fixed stabilizing beta-effect the exponential growth rate decreases to zero). With the small adaption in this case, the saturation bound near zero changes without large instability compared with the bound in Figure 4.1 with fixed $\beta=1$. Figure 4.3 shows the comparison between the numerical simulation results with the theoretical prediction

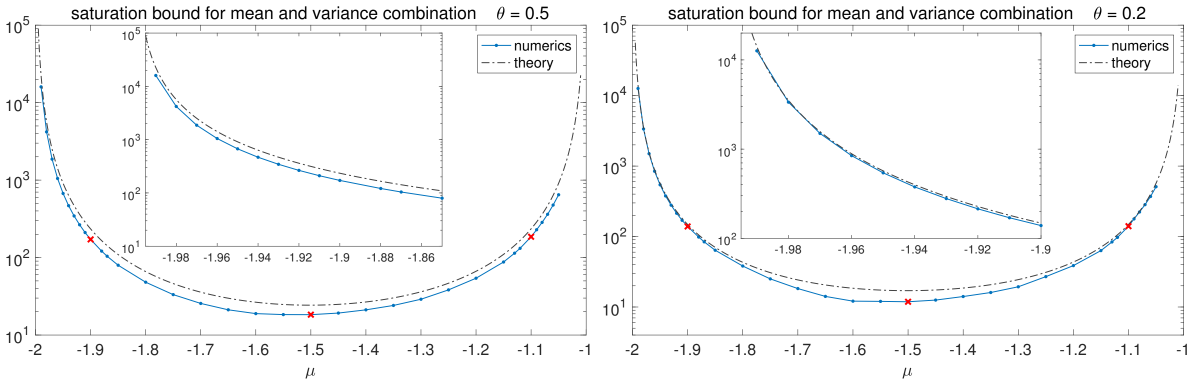


Fig. 4.2: Saturation bound in unstable regime $-2 < \mu < -1$ for statistical mean and variance combined with parameter $\theta$. The combined statistical energy $\theta E^m + E^v$ is compared with different ratio parameters $\theta = 0.5, 0.2$. The values for the typical flow fields in Section 2.3 with $\mu = -1.9, -1.5, -1.1$ are marked with a red cross.

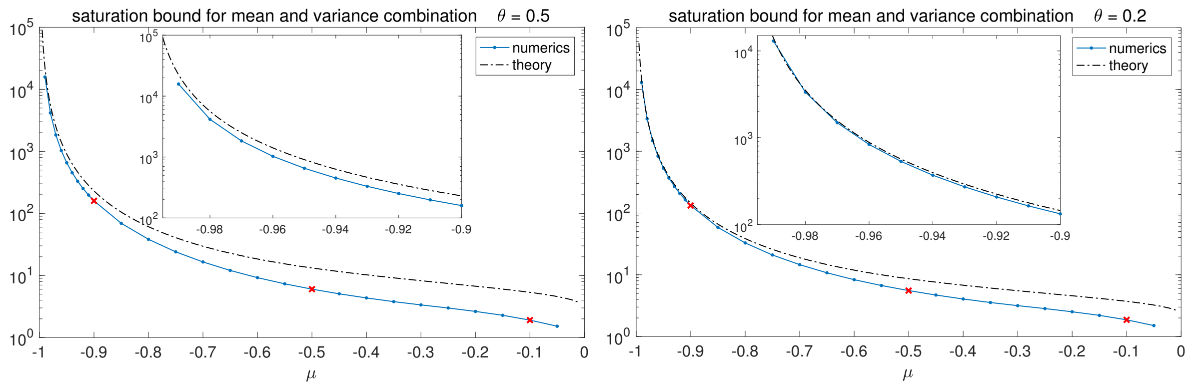


Fig. 4.3: Saturation bound in unstable regime $-1 < \mu < 0$ for statistical mean and variance combined with parameter $\theta$. The combined statistical energy $\theta E^m + E^v$ is compared with different ratio parameters $\theta = 0.5, 0.2$. The beta-effect is taken as $\beta = |\mu|$. The values for the typical flow fields in Section 2.3 with $\mu = -0.9, -0.5, -0.1$ are marked with a red cross.

as the parameter value changes. The theoretical saturation bound $C_\mu^\theta$ gives overall good estimation for the maximum statistical fluctuations that the system can reach with instability. Similar with the previous case, the saturation bound becomes extremely tight near the unstable point $\mu = -1$. With $\theta = 0.5$ the mean fluctuation gets more weight, and with $\theta = 0.2$ the variance is dominant and the bound becomes even tighter in estimating the total statistical variance in the ensemble. Near the other limit $\mu \to 0$ the instability vanishes. This is consistent with the linear analysis (see Appendix A) that no unstable growth takes place as $\mu \to 0$. The system can be stabilized from the interactions between the large and small scales through topographic stress at this point $\mu = 0$. Then the fluctuations in both statistical mean and variance decrease to small amount near this stable limit.

## 5 Statistical Saturation Bounds with Forcing and Dissipation

In our previous discussion, we focus on the the statistical bounds in mean fluctuation and variance dependent on the initial statistical configuration of the system without any external forcing and dissipation effects. Thus the total statistical energy is controlled by the initial state statistical mean and variance through the energy conservation principle. On the other hand, for the performance of the energy in the mean and variance in the long time limit, geometric ergodicity for the truncated topographic barotropic model (2.1) is proved under dissipation, inhomogeneous deterministic forcing and minimal stochastic forcing [23, 16]. Thus there exists an invariant measure that attracts all the solutions in the long time limit regardless of the initial values. In this section, we consider the statistical instability in this case with forcing and dissipation effects. Then the total statistical energy becomes no longer conserved due to the effect of forcing and dissipation. We will first consider the statistical energy equation in the stable regime $\mu > 0$, next the saturation bound can be found in a similar fashion as before.

### 5.1 The effects of additional deterministic and random external forcing in the stable regime

In the stable regime $\mu > 0$, we consider the effects from external forcing and damping to the total statistical energy dynamics in the mean and variance. In general, there could be a deterministic component and a stochastic component represented by Gaussian white noise in the forcing on both large mean flow and the vortical modes as in (2.12). The total statistical energy $E_\mu$ in fluctuation (2.10) then follows the dynamics (2.13) due to the Ekman damping and forcing effects

$$\frac{dE_\mu}{dt} = -2dE_\mu + \mu\bar{U}\cdot F_0 + \sum\left(1+\mu\left|\mathbf{k}\right|^{-2}\right)\hat{F}_{\mathbf{k}}^{*}\cdot\bar{\omega}_{\mathbf{k}} + Q_{\sigma,\mu},$$

with the deterministic part applying on the statistical mean state and the stochastic part offering the combined contribution through $Q_{\sigma,\mu}$. Now to find the upper bound of the total statistical energy during its evolution in time due to the external forcing, we need to separate the deterministic forcing with the mean state. First we have the inequality in the interaction terms with the statistical mean by applying Cauchy's inequality with parameter $\lambda > 0$

$$\begin{aligned}\left(1+\mu\left|\mathbf{k}\right|^{-2}\right)F_{\mathbf{k}}^{*}\cdot\bar{\omega}_{\mathbf{k}} &= \left|1+\mu\left|\mathbf{k}\right|^{-2}\right|^{1/2}F_{\mathbf{k}}^{*}\cdot\left|1+\mu\left|\mathbf{k}\right|^{-2}\right|^{1/2}\bar{\omega}_{\mathbf{k}}\\ &\leq \frac{1}{4\lambda}\left|1+\mu\left|\mathbf{k}\right|^{-2}\right|\left|\bar{\omega}_{\mathbf{k}}\right|^{2} + \lambda\left|1+\mu\left|\mathbf{k}\right|^{-2}\right|\left|F_{\mathbf{k}}\right|^{2}\\ &< \frac{1}{4\lambda}\left|1+\mu\left|\mathbf{k}\right|^{-2}\right|E_{\mathbf{k}} + \lambda\left|1+\mu\left|\mathbf{k}\right|^{-2}\right|\left|F_{\mathbf{k}}\right|^{2}.\\ \mu F_0\cdot\bar{U} &\leq \frac{1}{4\lambda}\left|\mu\right|\bar{U}^{2} + \lambda\left|\mu\right|F_0^{2} < \frac{1}{4\lambda}\left|\mu\right|E_U + \lambda\left|\mu\right|F_0^{2}.\end{aligned}$$

The above inequalities only hold for the stable regime $\mu > 0$ so that the coefficients on the right hand sides are always positive. Notice that $E_{\mathbf{k}} = \left\langle\left|\omega_{\mathbf{k}}\right|^{2}\right\rangle$ and $E_U = \left\langle U^2\right\rangle$ represent the total statistical energy including both mean fluctuation and variance in the vortical mode and the mean flow. The last inequality adds the variance to the original term containing purely the statistical mean. Thus the inflation at the last inequality could be large if the total variance makes a major contribution to the combined statistical energy.

Therefore we can define the *effective statistical forcing* $Q_{F,\mu}$ combining the contributions in deterministic and stochastic forcing all together

$$Q_{F,\mu}(\lambda) = \mu\left(\lambda F_0^2 + \frac{1}{2}\sigma_0^2\right) + \sum\left(1+\mu\left|\mathbf{k}\right|^{-2}\right)\left(\lambda\left|F_{\mathbf{k}}\right|^2 + \frac{1}{2}\sigma_{\mathbf{k}}^2\right), \quad \mu > 0;$$

and the *effective dissipation* in the statistical energy equation can be determined by changing the parameter value $\lambda$. The original system (2.13) already contains the Ekman damping $-2dE_\mu$, thus we can choose the parameter $\lambda > 0$ so long as there still exist a negative damping effect in the total statistical energy dynamics

$$\bar{d}_F(\lambda) = 2d - (2\lambda)^{-1} > 0, \quad \lambda > (8d)^{-1}.$$

For simplicity we could just take $2\lambda = d^{-1}$ so that $\bar{d}_F = d$. With all these arrangements we have the differential inequality for the total statistical energy $E_\mu$ from (2.13)

$$\frac{dE_\mu}{dt} \leq -\bar{d}_F E_\mu + Q_{F,\mu}.$$

Using Grönwall's inequality to the above relation we get the upper bound for the total statistical energy $E_\mu$ due to the effect of damping and external forcing

$$\begin{aligned} E_\mu(t) &\leq E_\mu(0)\, e^{-\bar{d}_F t} + \int_0^t e^{-\bar{d}_F(t-s)} Q_F(s)\, ds \\ &\leq \epsilon_T + \bar{d}_F^{-1} Q_{F,\mu}. \end{aligned} \tag{5.1}$$

Above the first inequality is for the general time-dependent case with the forcing effect, and the second one is under the further assumption of a constant forcing in time. The first component on the right hand side $\epsilon_T = E_{\mu,0}\exp\left(-\bar{d}_F T\right)$ gives one approximated decay rate of the initial statistics. If we just want to focus on the long time performance, the first term with initial statistics can be made arbitrarily small at the long time limit $t > T$, thus we need only focus on the second term above, that is,

$$Q_{F,\mu} = \mu\left(\frac{1}{2d}F_0^2 + \frac{1}{2}\sigma_0^2\right) + \sum\left(1+\mu\left|\mathbf{k}\right|^{-2}\right)\left(\frac{1}{2d}\left|F_{\mathbf{k}}\right|^2 + \frac{1}{2}\sigma_{\mathbf{k}}^2\right).$$

The stability can be developed in this forced-damped case in a similar way as before based on the inequality (5.1). Therefore we can summarize the stability result in the following theorem:

**Theorem 3.** *(Statistical energy bound with forcing and dissipation in the stable regime $\mu > 0$) Consider the forced-dissipated system (2.12) of fluctuations about the steady state solution $(V_\mu, Q_\mu)$. For any parameter value $\mu > 0$ the total statistical energy in the mean fluctuation and variance can be bounded by the inequality (5.1). Especially in the statistical steady state, the initial statistics get dissipated and the total statistical* *energy is determined by the external forcing and damping effects as*

$$E_{\mu}\left(t\right)\leq\frac{\mu}{2}\left(\left(d^{-1}F_{0}\right)^{2}+d^{-1}\sigma_{0}^{2}\right)+\frac{1}{2}\sum\left(1+\mu\left|\mathbf{k}\right|^{-2}\right)\left(\left|d^{-1}F_{\mathbf{k}}\right|^{2}+d^{-1}\sigma_{\mathbf{k}}^{2}\right).\tag{5.2}$$

Notice that (5.2) can be compared with the bound (3.1) from the non-forced non-damped case, where the deterministic forcing $d^{-1}F$ acts the similar role as the initial mean deviation and the stochastic forcing $\sigma^2$ acts as the role of the initial variance in the ensemble. The total statistical energy bound in long time limit can be calculated based on the forcing and damping parameters. Above in (5.2), we assume for simplicity that the deterministic forcing $F$ and stochastic forcing $\sigma$ are both independent in time. It should be easy to generalize the above bound to the time-dependent case.

### 5.2 Saturation bounds with forcing and dissipation in unstable regimes

In the unstable regime with $\mu<0$, just consider the special case of linear damping and forcing in the special form of (2.12) using equilibrium steady state without any additional terms $F_0=0, F=0$

$$\begin{aligned}\text{small scale}: &\quad -d\omega+d\bar{\omega}_{\mathrm{eq}}+\sigma_{\mathbf{k}}\dot{W}_{\mathbf{k}},\\ \text{large scale}: &\quad -dU+d\bar{U}_{\mathrm{eq}}+\sigma_{0}\dot{W}_{0}.\end{aligned}\tag{5.3}$$

The forcing structure above from equilibrium steady solution $\bar{\omega}_{\mathrm{eq},\mathbf{k}}=-\left|\mathbf{k}\right|^{2}\hat{\Psi}_{\mu,\mathbf{k}}$ and $\bar{U}_{\mathrm{eq}}=V_{\mu}$ is dependent on the parameter $\mu$. The statistical bound (5.2) for the stable regime $\mu>0$ enables us to carry out the same argument for initial state dependence in Section 4 to the forced-dissipated system in the same way. Again we can consider the saturation bound using a class of 'reference states' with parameters $\alpha>0$. Especially it is important to notice that the linear damping is applied on the fluctuation component according to the reference state $-dE_{\alpha}$. Using the reference state with parameter $\alpha$ but with the forcing in the form (5.3) with parameter $\mu$, the following additional forcing effects need to be added to the dynamical equation of $E_{\alpha}$ based on the reference state with parameter $\alpha$ in the mean flow and vortical modes

$$F_{0}=d\left(V_{\mu}-V_{\alpha}\right)\equiv dV_{\mu,\alpha},\quad F_{\mathbf{k}}=d\left(Q_{\mu,\mathbf{k}}-Q_{\alpha,\mathbf{k}}\right)\equiv dQ_{\mu,\alpha,\mathbf{k}}.$$

Assuming there is no additional forcing besides the above terms and using the inequality in (5.2), the statistical energy based on the reference state (4.5) can be recovered in this forced-dissipated case

$$\begin{aligned}2E_{\alpha}\left(t\right)&=\alpha\left[\left(V_{\mu,\alpha}+\bar{U}_{t}\right)^{2}+\overline{U_{t}^{\prime2}}\right]+\sum\left(1+\alpha\left|\mathbf{k}\right|^{-2}\right)\left[\left|Q_{\mu,\alpha,\mathbf{k}}+\bar{\omega}_{\mathbf{k},t}\right|^{2}+\overline{\left|\omega_{\mathbf{k},t}^{\prime}\right|^{2}}\right]\\&\leq2\bar{d}_{F}^{-1}Q_{F,\alpha}=\alpha\left(V_{\mu,\alpha}^{2}+d^{-1}\sigma_{0}^{2}\right)+\sum\left(1+\alpha\left|\mathbf{k}\right|^{-2}\right)\left(\left|Q_{\mu,\alpha,\mathbf{k}}\right|^{2}+d^{-1}\sigma_{\mathbf{k}}^{2}\right).\end{aligned}\tag{5.4}$$

This becomes a similar case with the previous non-forced non-damped situation in (4.8) with dependence on initial values. It is useful to notice that the random white noise forcing amplitude $(\sigma_0,\sigma_{\mathbf{k}})$ plays the same role as the initial ensemble variance in the unforced case; while the additional deterministic forcing with the equilibrium mean $\left(\bar{U}_{\mathrm{eq}}, \bar{\omega}_{\mathrm{eq}}\right)$ plays the role of the initial mean deviation in the previous unforced case (4.8). Therefore we can again find the saturation bound in the forced-damped case following the exact procedure as in Section 4.

*Saturation bound for total variance based on the kinetic energy*

The saturation bound for the total variance in the kinetic energy can be calculated by minimizing the right hand side of (5.4) among all the possible values of $\alpha > 0$ so that

$$C_{\mu}^{v}=\min_{\alpha>0}\left[\frac{(\alpha-\mu)^{2}}{\alpha^{2}}V_{\mu}^{2}+d^{-1}\sigma_{0}^{2}\right]+\sum_{1\leq|\mathbf{k}|\leq\Lambda}\left[\frac{(\alpha-\mu)^{2}|\mathbf{k}|^{2}}{\alpha\left(\alpha+|\mathbf{k}|^{2}\right)}\left|\Psi_{\mu,\mathbf{k}}\right|^{2}+\left(|\mathbf{k}|^{-2}+\alpha^{-1}\right)d^{-1}\sigma_{\mathbf{k}}^{2}\right],$$

with $V_{\mu}=-\beta/\mu$ and $\Psi_{\mu,\mathbf{k}}=\hat{h}_{\mathbf{k}}/\left(\mu+|\mathbf{k}|^{2}\right)$ the steady state solutions. The maximum total variance in the flow fluctuation with forcing and dissipation can be reached at

$$\overline{U_{t}^{\prime 2}}+\sum_{1\leq|\mathbf{k}|\leq\Lambda}|\mathbf{k}|^{2}\,\overline{|\psi_{\mathbf{k},t}^{\prime}|^{2}}\leq C_{\mu}^{v}\left(h,\beta,d,\sigma,\Lambda\right), \tag{5.5}$$

where the bound $C_{\mu}^{v}$ is dependent on the truncation size $\Lambda$, topographic structure $h$, the beta-effect $\beta$, Ekman friction rate $d$, and the stochastic forcing in each mode $\sigma$. Comparing this saturation bound $C_{\mu}^{v}$ with the previous case (4.10) in Section 4 with dependence on initial value, we find that the similar form can be reached in this forced-dissipated case. The deterministic forcing from the steady state solution can be compared with the initial mean state in the previous case, and the effective stochastic forcing amplitude $d^{-1}\sigma^{2}$ can be compared with the initial variance in the ensemble members.

*Saturation bound for total statistical fluctuations in a combination of energy in the mean and variance*

Similarly for the mean state including the differences in states $V_{\mu,\alpha}, Q_{\mu,\alpha}$ we have the estimation from Cauchy's inequality

$$\left(V_{\mu,\alpha}+\bar{U}\right)^{2}\geq\left(1-\epsilon^{-1}\right)V_{\mu,\alpha}^{2}+\left(1-\epsilon\right)\bar{U}^{2},$$
$$\left|Q_{\mu,\alpha,\mathbf{k}}+\bar{\omega}_{\mathbf{k}}\right|^{2}\geq\left(1-\epsilon^{-1}\right)\left|Q_{\mu,\alpha,\mathbf{k}}\right|^{2}+\left(1-\epsilon\right)\left|\bar{\omega}_{\mathbf{k}}\right|^{2}.$$

Substituting the above back to the original inequality (5.4), we can derive the saturation bound for a combination of the statistical mean fluctuation and variance

$$C_{\mu}^{\theta}=\min_{\alpha>0}\frac{1}{1-\theta}\left[\frac{(\alpha-\mu)^{2}}{\alpha^{2}}V_{\mu}^{2}+\sum\frac{(\alpha-\mu)^{2}|\mathbf{k}|^{2}}{\alpha\left(\alpha+|\mathbf{k}|^{2}\right)}\left|\Psi_{\mu,\mathbf{k}}\right|^{2}\right]+d^{-1}\left[\sigma_{U,0}^{2}+\sum\left(|\mathbf{k}|^{-2}+\alpha^{-1}\right)\sigma_{\mathbf{k},0}^{2}\right].$$

Then the combined statistical energy in the mean fluctuation and variance in the damped and forced case can be controlled by the upper bound $C_{\mu}^{\theta}$

$$\theta E^{m}\left(t\right)+E^{v}\left(t\right)\leq C_{\mu}^{\theta}\left(h,\beta,\sigma_{0},\Lambda\right), \tag{5.6}$$

with $\theta=1-\epsilon^{-1}<1$. Especially we can find the non-optimal bound for the statistical mean state as

$$\bar{U}_t^2+\sum_{1\leq|\mathbf{k}|\leq\Lambda}|\mathbf{k}|^2\left|\bar{\psi}_{\mathbf{k},t}\right|^2\leq C_\mu^m=\min_{\theta<1}\theta^{-1}\left(1-\theta\right)^{-1}C_\mu^v=4C_\mu^v. \tag{5.7}$$

Especially still in (5.6) we can even take $\theta<0$ to control the total variance in second order moments in the system from the totally energy in the mean fluctuation of the first order moments.

**Theorem 4.** *(Saturation bound for statistical mean and variance with damping and random forcing) With the special form of linear damping and forcing as in (5.3), the combined statistical mean fluctuation and variance, $\theta E^m+E^v$, with the ratio parameter $\theta<1$ can be controlled as in (5.6) with saturation bound $C_\mu^\theta$. Similarly the total variance in the flow fluctuation, $E^v$, is bounded by the saturation bound $C_\mu^v$ as in (5.5); and the total statistical energy in mean fluctuation, $E^m$, is bounded by the (non-optimal) bound $C_\mu^m=4C_\mu^v$.*

### 5.3 Numerical verification of the saturation bounds in the forced-dissipated case

Here again we check the saturation bounds derived in (5.5), (5.6), and (5.7) using numerical simulations in the statistically unstable regimes $-2<\mu<-1$. The basic setup is still kept the same as before with the same set of parameters in Section 2.3. Especially to make the bounds in the forced-dissipated case stay in the same form with the previous case, we apply the random forcing only on the mean flow $U$ and ground modes with $|\mathbf{k}|=1$ with noise amplitude and damping rate always in the consistent relation $d^{-1}\sigma^2\equiv\sigma_{\mathrm{eq}}^2=1$. So exactly the same saturation bounds can be used in this case. Besides we compare the mean and variance in statistical equilibrium state with different damping rates $d=0.05,0.1,0.25$. Typical flow structures in this forced-dissipated case has also been discussed in Figure 2.4 and Table 2 previous in Section 2.3. Notice that different damping and forcing strength can lead to distinct steady flow structures and statistics (for example, sometimes with opposite jet directions).

First in Figure 5.1 we show the statistical energy in the mean fluctuation and total variance separately with the the saturation bounds found in (5.5) and (5.7). Still the theoretical saturation bound provides proper estimation about the maximum statistical energy in both statistical mean and variance for all the different forcing and damping strengths especially near the resonance points $\mu\rightarrow-2,-1$. With larger uniform damping rate $d$ along all the scales (accordingly with larger stochastic forcing since we set $\sigma^2=d$) the total variance in the system increases; while the statistics in the mean decreases as the damping rate increases to suppress the mean fluctuation. This observation is consistent with intuition since the larger damping dissipates the mean fluctuation strongly to guarantee convergence to the mean steady state solution; and accordingly stronger random forcing injects more energy in the largest scales and then cascades throughout the scales. Correspondingly larger mean fluctuation and smaller variance will be induced with smaller damping rate $d$ and stochastic forcing $\sigma$.

Next Figure 5.2 compares the combined mean fluctuation and variance bounds with ratio parameter $\theta$ found in (5.6). In the combination of mean and variance together, unlike the previous plots with mean

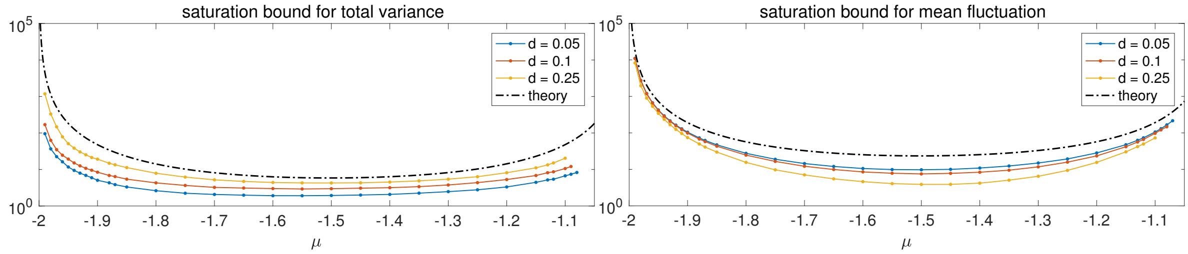


Fig. 5.1: Saturation bound with damping and forcing in the unstable regime $-2 < \mu < -1$ for statistical mean and variance separately. Results with different damping rates $d = 0.05, 0.1, 0.25$ are shown. The left panel compares the total variance $E^v$ and the right panel is the statistical energy in mean fluctuation $E^m$ (in solid lines) with the theoretical bounds $C^v_\mu, C^m_\mu$ (in dotted-dashed lines).

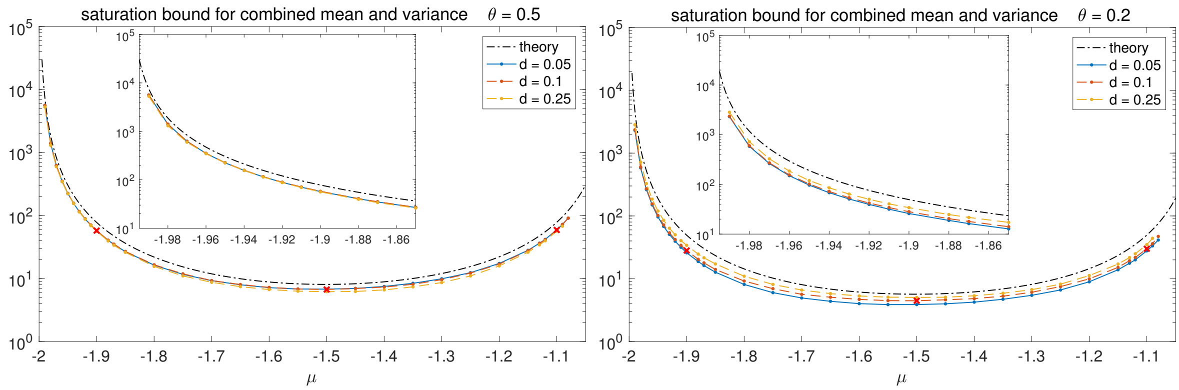


Fig. 5.2: Saturation bound with damping and forcing in the unstable regime $-2 < \mu < -1$ for statistical mean and variance combined with different $\theta$. The combined statistical energy $\theta E^m + E^v$ is compared with different ratio parameters $\theta = 0.5, 0.2$. Results with different damping rates $d = 0.05, 0.1, 0.25$ are shown. The values for the typical flow fields in Section 2.3 are marked with a red cross.

and variance separately, despite the differences in the statistical mean and variances with different damping rates, the total statistical energy in the three cases with different damping $d$ become near to each other and are close to the theoretical saturation bound uniformly. Similarly with the previous case we can observe the instability near $\mu \to -2$ is stronger than that near the other boundary $\mu \to -1$.

## 6 Further Discussion about the Statistical Bounds with Large-scale eigenmode Forcing and with the Total Enstrophy

We have derived the saturation bounds for the topographic barotropic flow depending on the initial statistics or on the external forcing and damping in a unified manner. Especially in the case with deterministic and stochastic forcing, we tested the bounds with deterministic forcing purely from the equilibrium steady state and the stochastic forcing on the largest scales as in (5.3). In this section, we offer some extensions about the previous statistical saturation bounds. First we discuss a more generalized forcing form with additional large-scale eigenmode forcing and random stochastic forcing on large scale modes; then both upper and lower saturation bounds are derived according to the statistical enstrophy in the vortical modes depending on the initial statistics.

### 6.1 The effect with eigenmode forcing on large scales

Here we consider a special and interesting form of the forced-dissipated system (2.12) with additional deterministic and stochastic forcing only applied on the largest spectral scales

$$\begin{aligned} \text{small scale :}\quad & -d\omega + d\bar{\omega}_{\text{eq}} + \mathcal{F}_1, \\ \text{large scale :}\quad & -dU + d\bar{U}_{\text{eq}} + \mathcal{F}_0. \end{aligned} \tag{6.1}$$

Above the additional $(\mathcal{F}_0, \mathcal{F}_1)$ in (6.1) are introduced as the *large-scale eigenmode forcing* [17] by adding both deterministic and random Gaussian components on the large scale mean flow $U$ and the vortical mode on ground energy shell with $|\mathbf{k}| = 1$

$$\mathcal{F}_1 = \sum_{|\mathbf{k}|=1} \left[F_{\mathbf{k}}(t) + \dot{W}_{\mathbf{k}}\sigma_{\mathbf{k}}(t)\right] e^{i\mathbf{k}\cdot\mathbf{x}}, \quad \mathcal{F}_0 = F_0(t) + \dot{W}\sigma_0(t).$$

This is the same form as tested in [27] for reduced order models. Under this large-scale forcing, energy is injected in the largest scales and then gets transferred down spectrum through the nonlinearity to the smaller scales to reach a final statistical steady state. In [17], deterministic nonlinear stability has been shown for the flow with the eigenmode forcing and linear damping without topographic stress. Here we discuss the statistical saturation bound with this large-scale eigenmode forcing and topography following the previous general framework.

In this case with additional deterministic forcing, the saturation bound in (5.4) will include one more term due to the injection of energy from $(F_0, F_1)$ on the largest scales. Therefore the total statistical energy based on the reference state $E_\alpha$ in (4.5) with $\alpha > 0$ follows the inequality

$$\begin{aligned} 2E_\alpha(t) \;\leq\; & \alpha\left(V_{\mu,\alpha} + d^{-1}F_0\right)^2 + \sum_{|\mathbf{k}|=1}(1+\alpha)\left(\left|Q_{\mu,\alpha,\mathbf{k}} + d^{-1}F_1\right|^2 + d^{-1}\sigma_1^2\right) \\ & + \alpha d^{-1}\sigma_0^2 + \sum_{|\mathbf{k}|^2\geq 2}\left(1+\alpha\left|\mathbf{k}\right|^{-2}\right)\left(\left|Q_{\mu,\alpha,\mathbf{k}}\right|^2\right). \end{aligned}$$

Above the first line contains the effects from the deterministic forcing on the large scale mean flow $U$ and the ground energy shell $|\mathbf{k}| = 1$. The second line is the contribution from all the other smaller scale modes the same as the previous case. Notice here in (6.1) we assume no random forcing on smaller scale modes $\sigma_{\mathbf{k}} \equiv 0, |\mathbf{k}| > 1$. Again remember that the total statistical energy $E_\alpha$ contains the differences with the reference states in the statistical mean so that we have the lower bound estimation as before in (4.11) to separate the statistical mean disturbance $\left(\bar{U}, \bar{\omega}\right)$ with the reference states difference $(V_{\mu,\alpha}, Q_{\mu,\alpha})$. In a similar way following the previous strategy as in (5.6) by minimizing among all the possible reference states with $\alpha > 0$, we find the saturation bound for the combination of the statistical energy in mean fluctuation $E^m$ and the total variance $E^v$ including the eigenmode forcing

$$\theta E^m + E^v \leq \min_{\alpha>0}\left[C_0^F + 4\left(\alpha^{-1}+1\right)C_1^F + C_2\right], \tag{6.2}$$

with $\theta < 1$. In the above inequality the first two constants $C_0^F$ and $C_1^F$ are related with the contributions from the large scale flow $U$ and the vortical ground modes subject to the eigenmode forcing in following explicit expressions

$$\begin{aligned} C_0^F &= \left(V_{\mu,\alpha} + d^{-1}F_0\right)^2 + \theta\left(1-\theta\right)^{-1} V_{\mu,\alpha}^2 + d^{-1}\sigma_0^2, \\ C_1^F &= \left|Q_{\mu,\alpha,1} + d^{-1}F_1\right|^2 + \theta\left(1-\theta\right)^{-1} \left|Q_{\mu,\alpha,1}\right|^2 + d^{-1}\sigma_1^2; \end{aligned} \tag{6.3}$$

and the last term $C_2$ is due to the contributions from all the other smaller scale modes without additional forcing in the consistent form with the saturation bound in the previous case

$$C_2 = \frac{1}{1-\theta} \sum_{|\mathbf{k}|^2 \geq 2} \frac{(\alpha-\mu)^2 |\mathbf{k}|^2}{\alpha\left(\alpha + |\mathbf{k}|^2\right)} \left|\Psi_{\mu,\mathbf{k}}\right|^2.$$

Comparing (6.2) with the previous saturation bounds in (5.6) without the eigenmode forcing, additional deterministic forcing effects $(F_0, F_1)$ adds contribution to the steady mean differences $(V_{\mu,\alpha}, Q_{\mu,\alpha})$. The ratio parameter $\theta < 1$ offers a weight in the total statistical mean component. With $\theta = 0$ the right hand side of (6.2) offers a saturation bound for the total variance; while as $\theta$ approaches 1 the second term on the right hand side of (6.3) goes up to infinity.

Previously in the saturation bounds, statistical instability always takes place at the resonance values $\mu = -|\mathbf{k}|^2$, where the mean state differences $(V_{\mu,\alpha}, Q_{\mu,\alpha})$ diverge to infinity as the parameter $\mu$ approaches the values $-|\mathbf{k}|^2$ for some wavenumber with $\hat{h}_{\mathbf{k}} \neq 0$. One interesting special choice of the eigenmode forcing is

$$F_0 = -dV_\mu, \quad F_1 = -dQ_{\mu,1}, \tag{6.4}$$

according to the steady state solution and making use of the steady differences, $V_{\mu,\alpha} = V_\mu - V_\alpha$, $Q_{\mu,\alpha} = Q_\mu - Q_\alpha$. Then the singularities in the first terms on the right hand sides of (6.3) in $C_0^F$ and $C_1^F$ get cancelled as $\left(V_{\mu,\alpha} + d^{-1}F_0\right)^2 = V_\alpha^2$, and $\left|Q_{\mu,\alpha,1} + d^{-1}F_1\right|^2 = \left|Q_{\alpha,1}\right|^2$ without any divergence of the upper bounds at the resonance point at $\mu = -1$. As a result the system gets stabilized due to this eigenmode forcing in the special form (6.4). Especially if we take $\theta = 0$ in (6.2) only the total variance is left on the left hand side. The total variance in the system with the special forcing (6.4) gets the saturation bound

$$\overline{U_t'^2} + \sum |\mathbf{k}|^2 \overline{|\psi_{\mathbf{k},t}'|^2} \leq \min_{\alpha>0} \left[\left(V_\alpha^2 + d^{-1}\sigma_0^2\right) + 2\left(\alpha^{-1}+1\right)\left(\left|Q_{\alpha,1}\right|^2 + d^{-1}\sigma_1^2\right) + C_2\right]. \tag{6.5}$$

Above on the right hand side of (6.5) the terms related with the steady state solution $(V_\mu, Q_{\mu,1})$ get cancelled entirely. Thus infinite saturation bound no longer exists at the limit $\mu \to -1$ with the additional balance forcing (6.4). The total variance $E^v$ gets a finite bound near the boundary as $\mu$ goes to $-1$. On the other hand with $\theta \neq 0$, there still exist singularities from the second terms on the right hand sides of (6.3). And the bounds blow up as a value of $\theta$ goes near 1. This implies that the total energy in mean fluctuations $E^m$ is still unbounded as $\mu$ approaches $-1$ even though we have finite variances $E^v$ in this case.

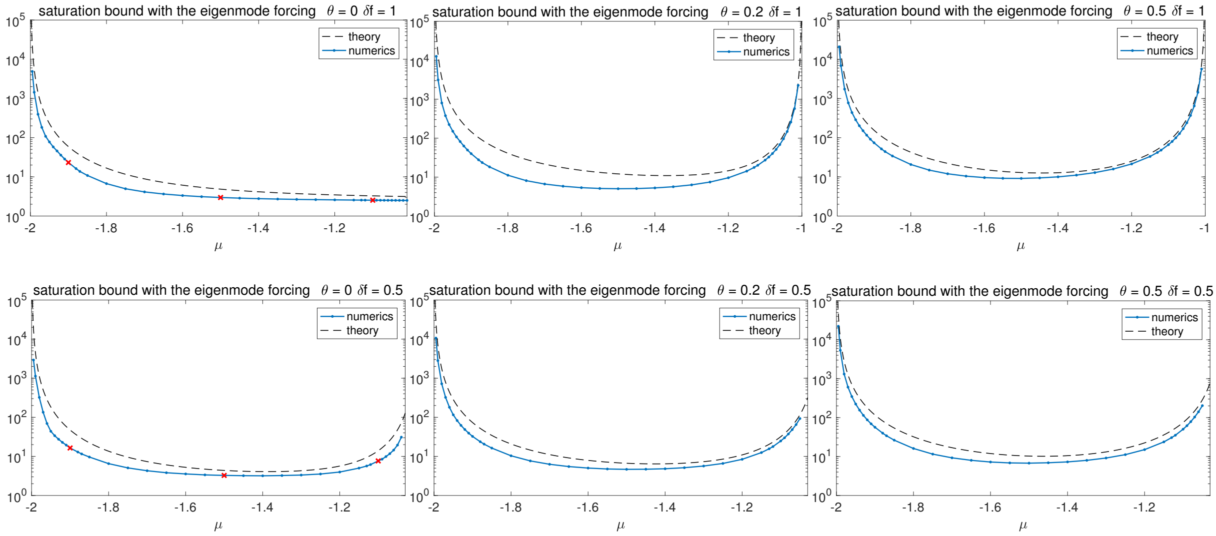


Fig. 6.1: Saturation bound for statistical mean and variance combined with the eigenmode forcing on the ground shell in the forms (6.6). The first line is with fully balanced forcing with strength $\delta f = 1$ and the second line is with $\delta f = 0.5$. The values for typical flow fields in Figure 2.5 with $\mu = -1.9, -1.5, -1.1$ are marked with a red cross.

### 6.1.1 *Numerical verification of the saturation bounds with large-scale eigenmode forcing*

In testing the saturation bound (6.2) and (6.5) with the large-scale eigenmode forcing, we still keep random white noise forcing only on the mean flow $U$ and ground modes with $|\mathbf{k}| = 1$ with noise amplitude and damping rate always in the relation $d^{-1}\sigma^2 \equiv \sigma_{\text{eq}}^2 = 1$; and we use intermediate linear damping rate $d = 0.1$. Especially we introduce the additional forcing in the form based on the steady state solution

$$F_0 = \delta f\left(-dV_\mu\right), \quad F_1 = \delta f\left(-dQ_{\mu,1}\right). \tag{6.6}$$

If we take the forcing strength $\delta f = 1$ this becomes the case in (6.4) that reduces the singularity at $\mu = -1$; and as a comparison we also test the case with $\delta f = 0.5$. The statistics from numerical simulations with $N = 1000$ particles are compared with the theoretical saturation bound in Figure 6.1. With $\theta = 0$ for the total variance in the system, near the limit $\mu = -2$ there still exists instability with the saturation bound goes to infinity due to the non-zero mode $\hat{h}_{(1,1)}$ and no additional eigenmode forcing on this mode. Near the other boundary at $\mu = -1$, the total variance stays in finite bound as predicted in (6.5) due to the balancing effect from the eigenmode forcing with $\delta f = 1$. In comparison with $\delta f = 0.5$, not all the singularity in the $|\mathbf{k}| = 1$ modes gets cancelled, thus the total variance increases again near $\mu = -1$ as shown in the second row of Figure 6.1. As we use non-zero value of $\theta$ the contribution from the statistical mean fluctuation is included, and the total statistics rise again near the boundary at $\mu = -1$ with $\delta f = 1$. This implies the instability in the mean fluctuation away from the original steady state solution $(V_\mu, Q_\mu)$ while the variance can be controlled in finite amount. Overall the saturation bounds still offer accurate estimation for the maximum amount of energy that the system can achieve due to the eigenmode forcing.

## 6.2 Upper and lower saturation bounds in statistical enstrophy

As another interesting special case we consider the statistical bounds in the eddy fluctuation modes $\omega$ only. In the statistics of the relative vorticity $\hat{\omega}_{\mathbf{k}}$ (compared with the stream functions $\hat{\psi}_{\mathbf{k}} = -|\mathbf{k}|^{-2}\hat{\omega}_{\mathbf{k}}$) larger emphasis is added on fluctuations in smaller scales. Especially if we want to calibrate the total statistics in mean and variance based on the enstrophy, $\mathcal{E} = \fint \left\langle \omega^2 \right\rangle$, only the statistics among the vortical modes are included. Notice that with the inclusion of mean flow interactions, the relative enstrophy is not conserved in the system and the large scale mean flow $U$ still has a crucial impact on the total statistical structure by transferring energy between different scales [17]. In this subsection we derive the statistical bounds for all the vortical modes based on the enstrophy $\mathcal{E}$. With no concern about the fluctuations in the large-scale mean flow, we can develop a lower bound on the total statistical enstrophy as well as the upper bound as before. Nevertheless the same strategy is also valid for the total kinetic energy $E$ used in the previous discussions.

Now we come back to the case depending on initial statistics with no external forcing and dissipation as in Section 4. Then the total statistical enstrophy $\mathcal{E} = \sum_{1\leq|\mathbf{k}|\leq\Lambda} |\bar{\omega}_{\mathbf{k}}|^2 + \overline{|\omega'_{\mathbf{k}}|^2}$ can be written according to the energy in the mean fluctuation and the variance in each model in the truncated system. Again the total statistical energy conservation (4.8) relates the statistics in the initial time with total energy in the later evolutions

$$E_\alpha^{\mathrm{stat}}(t) = \alpha\left[\left(V_{\mu,\alpha} + \bar{U}\right)^2 + \overline{U'^2}\right] + \sum\left(1 + \alpha|\mathbf{k}|^{-2}\right)\left[|Q_{\mu,\alpha,\mathbf{k}} + \bar{\omega}_{\mathbf{k}}|^2 + \overline{|\omega'_{\mathbf{k}}|^2}\right] = E_\alpha^{\mathrm{stat}}(0).$$

In fact the equality above is valid for all the values of $\alpha$, but the positive-definite condition for $E_\alpha^{\mathrm{stat}}$ might be violated when $\alpha < 0$. Previously we search among the solutions with $\alpha > 0$ so that $E_\alpha^{\mathrm{stat}}$ keeps positive definite. Now instead only the vortical modes $\hat{\omega}_{\mathbf{k}}$ are concerned so that we can extend to two parameter regimes $\alpha > 0$ and $-1 < \alpha < 0$. In these two regimes still the coefficients before the small scale modes $\omega_{\mathbf{k}}$ are all kept positive, $1+\alpha|\mathbf{k}|^{-2} > 0$ for all wavenumbers $\mathbf{k}$. Therefore we find the bounds for the total statistical energy conservation in statistical mean and variance among the vortical modes from two directions

$$\begin{aligned}
&\sum\left(1 + \alpha|\mathbf{k}|^{-2}\right)\left[|Q_{\mu,\alpha,\mathbf{k}} + \bar{\omega}_{\mathbf{k},t}|^2 + \overline{|\omega'_{\mathbf{k},t}|^2}\right] \leq E_\alpha^{\mathrm{stat}}(0), \quad \alpha > 0,\\
&\sum\left(1 + \alpha|\mathbf{k}|^{-2}\right)\left[|Q_{\mu,\alpha,\mathbf{k}} + \bar{\omega}_{\mathbf{k},t}|^2 + \overline{|\omega'_{\mathbf{k},t}|^2}\right] \geq E_\alpha^{\mathrm{stat}}(0), \quad -1 < \alpha < 0.
\end{aligned} \tag{6.7}$$

Above the first row in (6.7) is valid for $\alpha > 0$ and the second row is for $-1 < \alpha < 0$ since the sign in the large scale flow statistics $\alpha\left\langle U^2\right\rangle$ switches in the two regimes. On the right hand side the initial statistics $E_\alpha^{\mathrm{stat}}(0)$ still contain both information form the large scale mean flow $U$ and all the other vortical modes $\omega$ from the initial configuration of the ensemble

$$E_\alpha^{\mathrm{stat}}(0) = \alpha\left[V_{\mu,\alpha}^2 + \sigma_{U,0}^2\right] + \sum\left(1 + \alpha|\mathbf{k}|^{-2}\right)\left[|Q_{\mu,\alpha,\mathbf{k}}|^2 + \sigma_{\mathbf{k},0}^2\right].$$

In this way by focusing on the statistical energy in all the vortical modes only excluding the mean flow $U$ (and the statistics in the mean flow can be estimated from the saturation bounds in Section 4), we get the estimations of upper and lower bounds through (6.7). One final issue in the statistical mean part $|Q_{\mu,\alpha,\mathbf{k}}+\bar{\omega}_{\mathbf{k},t}|$, we need to separate the statistics in mean fluctuation from the steady state solution $Q_\mu$ by applying Cauchy's inequality once again to get the upper and lower bounds so that

$$\left(1-\epsilon^{-1}\right)|Q_{\mu,\alpha,\mathbf{k}}|^2+(1-\epsilon)|\bar{\omega}_{\mathbf{k},t}|^2\leq|Q_{\mu,\alpha,\mathbf{k}}+\bar{\omega}_{\mathbf{k},t}|^2\leq\left(1+\epsilon^{-1}\right)|Q_{\mu,\alpha,\mathbf{k}}|^2+(1+\epsilon)|\bar{\omega}_{\mathbf{k},t}|^2,$$

for any $\epsilon>0$. At last with $\alpha>-1$ the coefficients in front of each mode are all positive, $1+\alpha|\mathbf{k}|^{-2}>0$, and especially we can find the bounds in the coefficients $1+\alpha|\mathbf{k}|^{-2}\geq1+\alpha\Lambda^{-2}$ for $\alpha>0$ and $1+\alpha|\mathbf{k}|^{-2}\leq1+\alpha\Lambda^{-2}$ for $-1<\alpha<0$, with $|\mathbf{k}|\leq\Lambda$ the maximum truncation in the wavenumber. Combining everything together and following the same steps as in Section 4, the *saturation bounds in the total statistical enstrophy* can be developed as a combination in the statistical mean fluctuation and total variance according to the steady state with parameter $\mu$

$$\begin{aligned}\sum(1-\epsilon)|\bar{\omega}_{\mathbf{k}}|^2+\overline{|\omega'_{\mathbf{k}}|^2}&\leq C_\mu^U,\\\sum(1+\epsilon)|\bar{\omega}_{\mathbf{k}}|^2+\overline{|\omega'_{\mathbf{k}}|^2}&\geq C_\mu^L.\end{aligned}\tag{6.8}$$

Above $C_\mu^U,C_\mu^L$ are the upper and lower saturation bounds and $\epsilon>0$ is the weighting parameter controlling the statistical mean state. The upper bound is through the minimization of all $\alpha>0$ based on the first row of (6.7) and the lower bound is through the maximization of all $-1<\alpha<0$ on the second row,

$$\begin{aligned}C_\mu^U&=\min_{\alpha>0}\frac{V_{\mu,\alpha}^2+\sigma_{U,0}^2}{\alpha^{-1}+\Lambda^{-2}}+\sum\frac{1+\alpha|\mathbf{k}|^{-2}}{1+\alpha\Lambda^{-2}}\left(\epsilon^{-1}|Q_{\mu,\alpha,\mathbf{k}}|^2+\sigma_{\mathbf{k},0}^2\right),\\C_\mu^L&=\max_{-1<\alpha<0}\frac{V_{\mu,\alpha}^2+\sigma_{U,0}^2}{\alpha^{-1}+\Lambda^{-2}}+\sum\frac{1+\alpha|\mathbf{k}|^{-2}}{1+\alpha\Lambda^{-2}}\left(-\epsilon^{-1}|Q_{\mu,\alpha,\mathbf{k}}|^2+\sigma_{\mathbf{k},0}^2\right).\end{aligned}$$

Again unfortunately we cannot reach $\epsilon=0$ in the above estimations due to the term $\epsilon^{-1}$ in the saturation bounds. It is important to notice that on the right hand side of the upper bound $C_\mu^U$ every component is positive; while in the lower bound $C_\mu^L$ there is a negative term related with $|Q_{\mu,\alpha,\mathbf{k}}|$. Therefore the lower bound could become negative in value then has no control of the minimum amount of the statistical energy. Still as we will see in the numerical simulations next, in many situations a positive lower bound $C_\mu^L$ can be achieved thus it can serve as a tight estimation for the total statistical enstrophy in the system from the upper and lower estimation.

### *6.2.1 Numerical verification of the upper and lower saturation bounds in statistical enstrophy*

Finally we illustrate the upper and lower saturation bounds (6.8) in the total statistical enstrophy through numerical simulations. In this case without external forcing and damping the final statistics are again dependent on the initial statistical setup. As in the tests in Section 4 we assume no bias in the initial mean, $\bar{U}_0=0,\bar{\omega}_0=0$, from the steady state solution $(V_\mu,Q_\mu)$; and the initial ensemble variance is added to the

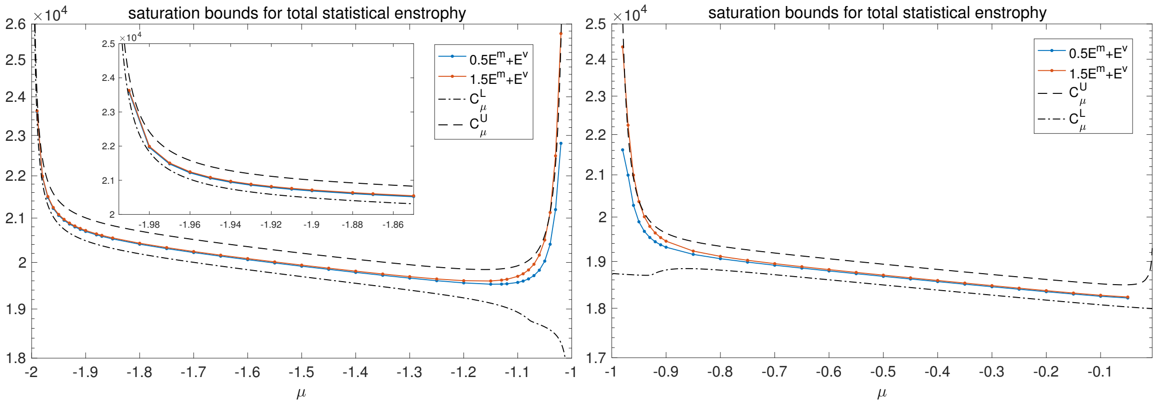


Fig. 6.2: Statistical saturation bounds compared with numerical simulations for total statistical enstrophy $\mathcal{E} = \fint \langle \omega^2 \rangle$ in regimes $-2 < \mu < -1$ and $-1 < \mu < 0$. We choose $\epsilon = 0.5$ in the upper and lower bounds $C_\mu^U, C_\mu^L$.

stable small scale modes this time with amplitudes

$$\sigma_{\mathbf{k}} = \sigma_{\text{eq}} \left(1 + \mu \left|\mathbf{k}\right|^{-2}\right)^{-1}, \quad \text{if } 1 + \mu \left|\mathbf{k}\right|^{-2} > 0.$$

The noise amplitudes $\sigma_{\mathbf{k}}$ are determined according to the equilibrium invariant measure (2.6) in the stable regime. Here we test the unstable regime with $\mu < 0$. Thus there exists inverse cascades of the statistical energy to the large scales due to nonlinear interactions. In this setup of the initial statistics the contribution from the random noise is larger compared with the negative component $\epsilon^{-1} \left|Q_{\mu,\alpha,\mathbf{k}}\right|^2$ in the lower bound $C_\mu^L$ so that it is easier to find a positive lower bound. Furthermore we use the single-mode topography $h = H(\sin x + \cos x)$ without smaller scale structures.

In Figure 6.2 we compare the upper and lower saturation bounds in total enstrophy with numerical simulations among test regimes $-2 < \mu < -1$ and $-1 < \mu < 0$. We choose $\epsilon = 0.5$ in (6.8) for the tests, so $0.5\mathcal{E}^m + \mathcal{E}^v$ is bounded from the upper side with $C_\mu^U$ and $1.5\mathcal{E}^m + \mathcal{E}^v$ is bounded from the lower side with $C_\mu^L$. Notice due to numerical dissipation in the system, the numerical results may become smaller than the real total statistics in the system with no explicit damping and forcing. First an extremely tight bound from upper and lower side can be achieved near $\mu = -2$. The total statistical energy in enstrophy is constrained inside the small band predicted by the saturation bounds in both directions. Among a wide range of values away from the singular points $\mu = -2, -1$, the saturation bounds offer good and tight estimates from above and below, setting a general accurate prediction for the maximum and minimum amount of energy the system can achieve according to different reference states with $\mu$. At last the lower bound goes to negative values at the resonance point $\mu = -1$ thus cannot offer a good estimation from below. But still the upper bound gives an accurate maximum total statistics bound in the enstrophy in both regimes.

## 7 Summary

In this paper, we developed rigorous statistical bounds for the saturation of instabilities about fluctuations in statistical mean and variance in the truncated barotropic equations over topography. Different from the deterministic nonlinear stability [6, 3, 17] that tracks the development of perturbations in time along one trajectory realization of the turbulent flow solutions, the statistical stability in uncertainty quantification takes into account the time evolution of both statistical mean fluctuation and variance from an ensemble representation. The statistical description about the system can offer a more comprehensive characterization about the nonlinear instabilities in ensemble statistics rather than only a pointwise quantification about the fluctuations in time around the steady state attractor. Direct numerical simulations as well as the transient statistical instability analysis about the linearized covariance equation (in Appendix A) reveal strong turbulent and unstable phenomena in the topographic barotropic flows, such as changing directions of the westward to eastward zonal jets, in general among a wide range of parameter regimes.

The statistical stability analysis is based on the statistical energy conservation principle [16, 18, 17] about the pseudo-energy in the fluctuation equations of the barotropic turbulence about steady state basic flows. The steady state solutions can be categorized into a statistically stable regime where the total statistical energy is positive-definite with a direct upper bound; and a statistically unstable regime where only a slaving principle for relations between statistical energy between small and large scale modes is available [17]. The focus is on finding a uniform saturation bound especially among the statistically unstable regimes. Using the idea in the saturation of deterministic instability from [29], we derive the statistical saturation bounds for both statistical mean fluctuation and variance in the unstable regimes by referring to a class of statistically stable states with explicit statistical upper bounds due to statistical energy conservation. The saturation bounds then can be achieved by minimization among all the bounds from the stable solutions. Typically two different types of uncertainties are discussed: the first case considers the dependence on the initial ensemble mean bias and the ensemble variance for a system without external forcing and dissipation; the second case instead includes Ekman damping and additional deterministic and random white noise forcing to the system and investigates the saturation bounds in the statistical equilibrium. With simple restrictions on the structure of the deterministic forcing, the saturation bounds in the two situations are developed under a uniform framework based on the statistical energy conservation of fluctuations. As some further applications of the general statistical stability analysis method, we also discuss special saturation bounds with the effect of large-scale eigenmode forcing where the instability in the total variance at the largest scale mode can be suppressed with proper choice of the forcing; and with the upper and lower bounds in the total statistical enstrophy for the statistics in small scale eddies to offer a tight constraint for the statistical variability from both sides. Overall the theoretical saturation bounds offer accurate estimation about the maximum statistical fluctuations in all the test regimes. At last, the extension of the present statistical bounds to more general systems for turbulence on the sphere or multilayer models with baroclinic instability [15, 26, 17, 9] creates additional challenges in future works.

**Acknowledgements** This research of the A. J. M. is partially supported by the Office of Naval Research through MURI N00014-16-1-2161 and DARPA through W911NF-15-1-0636. D. Q. is supported as a postdoctoral fellow on the second grant.

# A Transient Statistical Instability of the Barotropic System with Topography

In this appendix we illustrate the transient statistical instability existing generally in the topographic barotropic flows from the linearized statistical equations. It can be seen that the system contains strong internal growth of uncertainty among a wide parameter regimes despite the saturated statistical stability bounds achieved in the main text. In the transient statistical stability analysis, we calculate the maximum growth rate in the covariance equation near a statistically steady state solution. The positive growth rate characterizes the increase in uncertainty represented by the ensemble variance. Typically this can illustrate the exponential growth of the ensemble 'spread' in the transient state with a Gaussian initial distribution assigned to the group of particles.

In the barotropic flow with topography, the instability is mainly due to the energy transfer between the large-scale flow $U$ and the small-scale eddies $\omega$. For simplicity in analysis it is useful to consider the *layered topographic modes* [17] only along $x$-direction

$$h=\sum_{k=-N}^{N}\hat{h}_k e^{ikx},\qquad \omega=\sum_{k=-N}^{N}\hat{\omega}_k e^{ikx}.$$

The above layered modes with wavenumbers $\mathbf{k}=(k,0)$ form a closed system. The quadratic nonlinear interactions in (2.7) between small-scale layered modes, $\nabla^{\perp}\psi\cdot\nabla\omega$ and $\nabla^{\perp}\Psi\cdot\nabla\left(\omega-\mu\psi\right)$, are eliminated since all the wavenumbers are along the same direction. This simplification enables us to focus on the interactions between the large mean flow and small scale modes due to topographic stress and beta-effect. Therefore the original fluctuation equation can be effectively simplified in the spectral domain as

$$\begin{aligned}\frac{d\hat{\omega}_k}{dt}&=i\beta\frac{\mu+k^2}{\mu k}\hat{\omega}_k-i\frac{\mu k}{\mu+k^2}\hat{h}_kU\left(t\right)-ik\hat{\omega}_kU\left(t\right),\\ \frac{dU}{dt}&=\sum_{k=-N}^{N}\frac{\hat{h}_k^*}{ik}\hat{\omega}_k.\end{aligned}\tag{A.1}$$

Notice that the state variables $(U,\omega)$ in (A.1) are already the fluctuation components about the steady state solution $(V_\mu,Q_\mu)$ defined in (2.4). The nonlinear coupling between the mean flow and vortical modes is from the last term in the first equation. The chaotic dynamics with deterministic instability in the layered model is discussed in Chapter 5 of [17]. Next we consider the statistical growth rate in the transient state from an Gaussian initial distribution due to the instability from topography using the layered model (A.1).

## A.1 Transient statistical instability in the layered model

We investigate the statistical instability from the statistical formulation of the layered system (A.1), where no nonlinear interactions between small scale modes are included. Thus the only source of instability is from the interaction between large and small scales due to the topographic stress $h$. For a better formulation of the linearized system, we decompose the complex spectral modes into the real and imaginary part

$$\hat{\omega}_k=a_k+ib_k,\quad \hat{h}_k=h_k^r+ih_k^i,\qquad k=1,\cdots,N,$$

with $\hat{\omega}_{-k} = \hat{\omega}_k^*, \hat{h}_{-k} = \hat{h}_k^*$. Thus the state variables of interest form the vector $\mathbf{u} = (a_1, b_1, \cdots, a_N, b_N, U)^T$ of length $2N+1$. From the layered equation (A.1) the deterministic dynamics of each wavenumber $k$ can be written as

$$\begin{aligned}
\frac{da_k}{dt} &= -\beta\frac{\mu+k^2}{\mu k}b_k + \frac{\mu k}{\mu+k^2}h_k^i U + kb_kU,\\
\frac{db_k}{dt} &= \beta\frac{\mu+k^2}{\mu k}a_k - \frac{\mu k}{\mu+k^2}h_k^r U - ka_kU,\\
\frac{dU}{dt} &= 2\sum_{k=1}^{N}k^{-1}\left(h_k^r b_k - h_k^i a_k\right).
\end{aligned} \tag{A.2}$$

The small scale spectral modes $(a_k, b_k)$ are decoupled with each other in (A.2), while the mean flow $U$ combines all the feedbacks from small scales through the topographic stress. The only nonlinearity of the above system comes from the mean flow and vortical modes interactions, $(a_kU, b_kU)$.

To consider the statistical evolution of uncertainty in the system (A.2), it is useful to derive the dynamical equation of the covariance matrix $R = \left\langle \mathbf{u}'\mathbf{u}'^T\right\rangle$ for fluctuations $\mathbf{u}'$ away from a statistically steady mean state $\bar{\mathbf{u}}_k = \left(\bar{a}_k, \bar{b}_k, \bar{U}\right)$. The exponential growth rate of the linearized covariance $R$ illustrates how the uncertainty from the initial data grows due to the instability in the system; and the statistical mean state is the fixed point that a steady state solution can be reached. The linearized part of the covariance dynamics for $R$ can be written abstractly as

$$\frac{dR}{dt} = L_{\bar{\mathbf{u}}}R + RL_{\bar{\mathbf{u}}}^T + h.o.t.,\quad R = R^T = \begin{bmatrix} \ddots & & & & \vdots\\ & \overline{a_k'^2} & \overline{a_k'b_k'} & \cdots & \overline{a_k'U'}\\ & \overline{b_k'a_k'} & \overline{b_k'^2} & & \overline{b_k'U'}\\ & \vdots & & \ddots & \vdots\\ \cdots & \overline{U'a_k'} & \overline{U'b_k'} & \cdots & \overline{U'^2}\end{bmatrix}_{(2N+1)\times(2N+1)}.$$

Above $h.o.t.$ represents the third-order moment feedbacks to the covariance (see details as in [19,20]). In the linear statistical stability analysis, we assume a Gaussian distribution in the initial ensemble so the third-order moments are zero initially, and observe the growth in the covariance matrix in the transient state. Thus the effects of higher order moments are small in the beginning time. The linearized coefficient $L_{\bar{\mathbf{u}}}$ related with the statistical mean state $\bar{\mathbf{u}}$ can be written in a block-diagonal structure in the small scale modes

$$L_{\bar{\mathbf{u}}} = \begin{bmatrix} \ddots & & & 0 & \vdots\\ & 0 & -\beta\frac{\mu+k^2}{\mu k}+k\bar{U} & \cdots & \frac{\mu k}{\mu+k^2}h_k^i + k\bar{b}_k\\ & \beta\frac{\mu+k^2}{\mu k}-k\bar{U} & 0 & & -\frac{\mu k}{\mu+k^2}h_k^r - k\bar{a}_k\\ 0 & & \vdots & \ddots & \vdots\\ \cdots & -2k^{-1}h_k^i & 2k^{-1}h_k^r & \cdots & 0\end{bmatrix}_{(2N+1)\times(2N+1)}. \tag{A.3}$$

Therefore the linear instability can be characterized by the positive eigenvalues of the linearized coefficient matrix $L_{\bar{\mathbf{u}}}$. The positive eigenvalues illustrate the exponential growth rate of the uncertainty in covariance from the initial Gaussian ensemble around the presumed steady state statistical mean $\bar{\mathbf{u}} = \left(\bar{a}_k, \bar{b}_k, \bar{U}\right)$ (a relation in the mean states is proposed next based on the steady state mean equations). Large growth rate implies that the growing uncertainty in variances may drive the system to diverge from the original statistical mean $\bar{\mathbf{u}}$. Especially if we set zero mean state $\bar{a}_k = \bar{b}_k = \bar{U} = 0$, the eigenvalues of the above matrix $L_{\bar{\mathbf{u}}}$ are the same with the local Lyapunov exponents of the original linearized system (A.2) that characterize the separation rate of two trajectories with close initial states.

### *A.1.1 Transient growth rate in single mode interaction*

We begin with the simple setup that there is one single non-zero topographic mode $\hat{h}_k$ and small scale mode $(a_k, b_k)$ interacting with the mean flow $U$. Then all the other modes $(a_l, b_l)$ with $l \neq k$ remain zero for all the time from the decoupled dynamics in (A.2) (see Chapter 5 of [17]). Therefore the linearized coefficient matrix $L_{\bar{\mathbf{u}},k}$ becomes just a $3\times 3$ matrix

$$L_{\bar{\mathbf{u}},k} = \begin{bmatrix} 0 & -\beta\frac{\mu+k^2}{\mu k} + k\bar{U} & \frac{\mu k}{\mu+k^2} h_k^i + k\bar{b}_k \\ \beta\frac{\mu+k^2}{\mu k} - k\bar{U} & 0 & -\frac{\mu k}{\mu+k^2} h_k^r - k\bar{a}_k \\ -2k^{-1}h_k^i & 2k^{-1}h_k^r & 0 \end{bmatrix}.$$

Furthermore, we consider a special form of topography with only non-zero imaginary part

$$h_k^r \equiv 0,\ h_k^i = H \ \Rightarrow\ \bar{a}_k \equiv 0,\ \bar{b}_k = \frac{\frac{\mu k}{\mu+k^2}\bar{U}}{\frac{\beta}{\mu}\frac{\mu+k^2}{k} - k\bar{U}} H.$$

The coefficient matrix $L_{\bar{\mathbf{u}},k}$ first has one zero eigenvalue $\lambda = 0$, and the other two eigenvalues can be solved by

$$\begin{aligned} \lambda^2 &= -\left(\frac{\beta}{\mu}\frac{k^2+\mu}{k} - k\bar{U}\right)^2 - 2H\left(\frac{\mu}{k^2+\mu}H + \bar{b}_k\right) \\ &= 2H^2\left[k^2\bar{U}/\beta - \left(1+\mu^{-1}k^2\right)\right]^{-1} - \left(\frac{\beta}{\mu}\frac{k^2+\mu}{k} - k\bar{U}\right)^2. \end{aligned} \tag{A.4}$$

Statistical instability takes place when the right hand side above is positive. We can first find an immediate result that a necessary condition for the existence of linear instability occurs when

$$k^2\bar{U}/\beta - \left(1+\mu^{-1}k^2\right) > 0 \ \Leftrightarrow\ \bar{U} + V_\mu > \beta k^{-2},$$

in the northern hemisphere $\beta > 0$. This shows a lower bound for the total mean flow $\bar{U} + V_\mu$ to induce instability. The growth rate with single mode interaction will also be illustrated through numerical results next.

As one specific example, we consider the case with zero steady mean state, $\bar{a}_k = \bar{b}_k = \bar{U} = 0$. The eigenvalues (Lyapunov exponents) in (A.4) can be simplified as

$$\lambda^2 = -\frac{2H^2}{1+\mu^{-1}k^2} - \beta^2\left(\frac{k}{\mu} + \frac{1}{k}\right)^2.$$

Explicitly we can calculate the regime of linear instability among the values of

$$-k^2 < \mu < -\left[\left(\frac{2H^2}{\beta^2}\right)^{\frac{1}{3}} k^{-4/3} + k^{-2}\right]^{-1} \equiv \mu_c. \tag{A.5}$$

The growth rate $\lambda \to \infty$ as $\mu \to -k^2$; and the growth rate $\lambda \to 0$ as $\mu \to \mu_c$. Obviously the beta-effect works as a stabilizing effect so that larger value of $\beta$ makes smaller regime of instability. On the other hand, the larger values of the topographic strength $H$ will induce stronger instability into the system when the system becomes unstable. (A.5) is consistent with the deterministic linear instability discussed in Chapter 5 of [17].

### *A.1.2 Relations in the statistical steady mean state*

Here we propose a special set of values in the statistical mean $\left(\bar{a}_k, \bar{b}_k, \bar{U}\right)$ for calculating the transient growth rate from the steady state solution of the mean equations. The statistical mean dynamics can be derived by taking ensemble average about the original equations (A.2) so that

$$\begin{aligned}\frac{d\bar{a}_k}{dt} &= -\beta\frac{\mu+k^2}{\mu k}\bar{b}_k + \frac{\mu k}{\mu+k^2}h_k^i\bar{U} + k\bar{b}_k\bar{U} + k\overline{b_k'U'},\\ \frac{d\bar{b}_k}{dt} &= \beta\frac{\mu+k^2}{\mu k}\bar{a}_k - \frac{\mu k}{\mu+k^2}h_k^r\bar{U} - k\bar{a}_k\bar{U} - k\overline{a_k'U'},\\ \frac{d\bar{U}}{dt} &= 2\sum_{k=1}^{N}k^{-1}\left(h_k^r\bar{b}_k - h_k^i\bar{a}_k\right).\end{aligned}$$

In statistical steady state, the time derivatives on the left hand side vanish. Especially, we assume a statistical steady state under the *homogeneous assumption* that there is no cross-covariance in the steady state and the mean flow dynamics vanish at each mode

$$h_k^i\bar{a}_k = h_k^r\bar{b}_k, \quad \overline{a_k'U'} = \overline{b_k'U'} = 0,$$

which can also be guaranteed automatically from the initial setup. The above relations assume a homogeneous steady state without cross-covariances between modes in different scales. With the assumptions, the statistical mean of each small-scale mode can be determined by the large-scale flow mean $\bar{U}$,

$$\bar{a}_k = \frac{\frac{\mu k}{\mu+k^2}\bar{U}}{\frac{\beta}{\mu}\frac{\mu+k^2}{k} - k\bar{U}}h_k^r, \quad \bar{b}_k = \frac{\frac{\mu k}{\mu+k^2}\bar{U}}{\frac{\beta}{\mu}\frac{\mu+k^2}{k} - k\bar{U}}h_k^i, \tag{A.6}$$

The group of steady state means (A.6) from the homogeneous assumption may not be unique. We adopt this kind of solutions to illustrate the instability features of the system as a typical example.

## A.2 Numerical illustration of the statistical instability with exponential growth rate

In this part, we further illustrate the transient statistical instability analyzed above with simple numerical results. We compare the exponential growth rates from both the single topography interaction and the full linearized coefficient matrix $L_{\bar{\mathbf{u}}}$ in (A.3) where mean flow interaction with multiple small scale spectral modes is included.

### *A.2.1 Transient growth rate with zero mean fluctuation*

First we consider the case with zero steady mean fluctuation, $\bar{a}_k = \bar{b}_k = \bar{U} = 0$. The exponential growth here illustrates the increase in the variance from an initial Gaussian distribution with no bias in the mean. Figure A.1 shows the exponential growth rates from interactions with the leading four wavenumbers $k = 1, 2, 3, 4$. The layered topographic is taken as $\hat{h}_k = Hk^{-2}e^{-i\theta_k}$ in each spectral mode with uniform phase shift $\theta_k = \frac{\pi}{4}$ in the same zonal structure as in the main text. In the single mode interaction case, consistent with the analysis result in (A.5), large exponential growth will be induced when the parameter $\mu$ reaches the resonance points $-k^2$, and instability vanishes after the critical value $\mu_c$. Also notice that there exists overlap between the unstable regimes of different wavenumbers.

We also compute the maximum eigenvalue directly from the full linearized coefficient matrix (A.3) in the dotted-dashed line in Figure A.1. In this case, the feedbacks to the mean flow from each small scale mode are combined together. Again the growth rate becomes large near the resonance points $\mu = -k^2$. And the growth rate gets reduced among the overlapped regimes of different single mode instability. In the regime $-1 < \mu < 0$ interactions with other smaller scale modes has little effect on the final growth rate with single mode interaction. Especially note that the unbounded growth rate is one-sided. Positive growth rate only appear when $\mu$ approaches $-k^2$ from the right side, while weaker instability is generated from the left side. Similar phenomena can be observed from the model simulations for statistical instability in the main text.

The effect with different values of $\beta$ in the linear stability is shown in the right panel in Figure A.1. Here we test different values $\beta = 0, 0.1, 0.5, 1, 5$. Consistent with the results before, the beta-effect can serve as a stabilizing factor. As the value

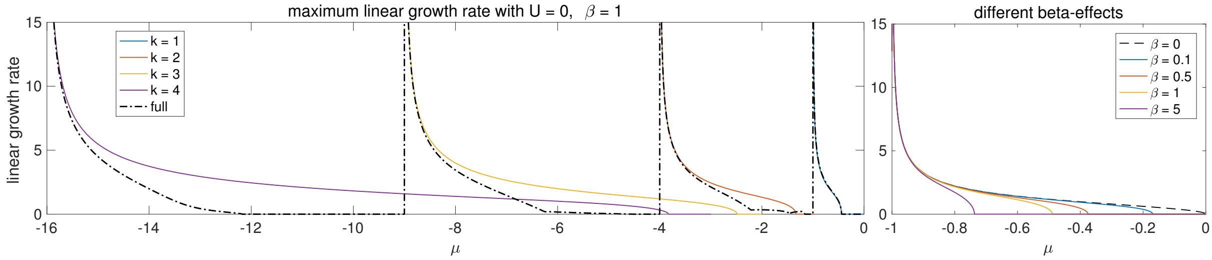


Fig. A.1: Transient growth rate from the largest positive eigenvalue of the linearized coefficient matrix in the covariance equation with $\beta = 1, \bar{U} = 0$. The four solid lines are the growth rates from single mode interaction with wavenumber $k = 1, 2, 3, 4$ separately as in (A.4). The dotted-dashed line is from the combined interaction of the full matrix (A.3) of all first four modes. The right panel shows results with different values of $\beta = 0, 0.1, 0.5, 1, 5$.

of $\beta$ increases, the size of the unstable regime with a positive growth rate gets reduced, while the entire regime $-1 < \mu < 0$ is unstable when $\beta = 0$.

### *A.2.2 Transient growth rate with non-zero mean fluctuation*

Further we show the statistical growth rate with non-zero mean state $\bar{U} \neq 0$. In Figure A.2a, as a further comparison, we show the exponential growth rate of multiple modes interaction with dependence on steady state mean flow value $\bar{U}$. Compared with the previous case with zero mean state $\bar{U} = 0$, positive exponential growth rates are also induced in the statistically nonlinear stable regime $\mu > 0$. The various regimes of positive growth rates show the large instability existing with the topographic barotropic flow in the general sense.

Further in Figure A.2b, we plot the regimes of unstable growth rates with different steady mean values $\bar{U}$ and parameter $\mu$. As the wavenumber $k$ increases, the unstable regime becomes narrower. As the steady mean state $|\bar{U}|$ increases, the instability reduces and finally vanishes. And especially in regime $\bar{U} > 0$, there exist two separated regimes for $\mu > 0$ and $\mu < 0$ with positive growth rates. Comparing with the single mode $k = 1$ case, the unstable regime with positive exponential growth rate gets narrowed down by including multiple small-scale mode interactions. Still the two branches of transient statistical unstable regimes exist.

## References

1. Anderson, J.L., Stern, W.F.: Evaluating the potential predictive utility of ensemble forecasts. Journal of climate **9**(2), 260–269 (1996)
2. Bakas, N.A., Ioannou, P.J.: Structural stability theory of two-dimensional fluid flow under stochastic forcing. Journal of Fluid Mechanics **682**, 332–361 (2011)
3. Bouchet, F., Venaille, A.: Statistical mechanics of two-dimensional and geophysical flows. Physics reports **515**(5), 227–295 (2012)
4. Buizza, R., Palmer, T.N.: Impact of ensemble size on ensemble prediction. Monthly Weather Review **126**(9), 2503–2518 (1998)
5. Cai, D., Haven, K., Majda, A.J.: Quantifying predictability in a simple model with complex features. Stochastics and Dynamics **4**(04), 547–569 (2004)
6. Carnevale, G.F., Frederiksen, J.S.: Nonlinear stability and statistical mechanics of flow over topography. Journal of Fluid Mechanics **175**, 157–181 (1987)
7. David, T.W., Marshall, D.P., Zanna, L.: The statistical nature of turbulent barotropic ocean jets. Ocean Modelling **113**, 34–49 (2017)

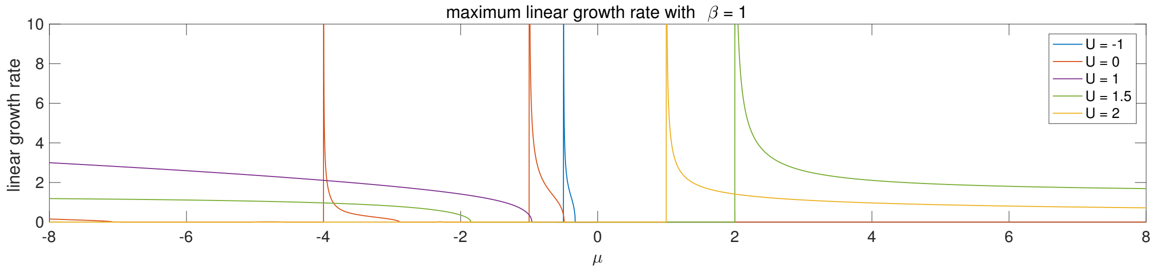


(a) Transient growth rates with first four modes interacting with different $\bar{U}=-1,0,0.5,1.5$

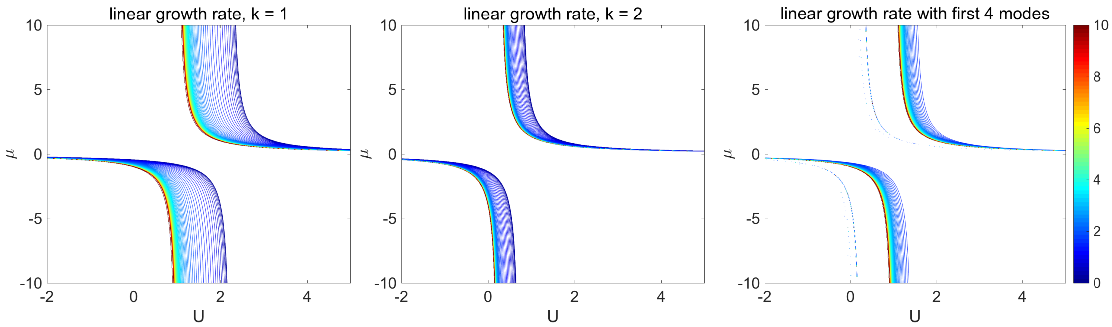


(b) Transient growth rates with changing steady mean state $\bar{U}$ and parameter $\mu$

Fig. A.2: Transient growth rates from the largest positive eigenvalue of the linearized coefficient matrix in the covariance equation with changing $\bar{U}=-1,0,0.5,1.5$. The second row shows the exponential growth rates with changing steady mean state $\bar{U}$ and parameter $\mu$ with $\beta=1$. The interactions with first two wavenumbers $k=1,2$ are shown separately.

8. Ehrendorfer, M., Tribbia, J.J.: Optimal prediction of forecast error covariances through singular vectors. Journal of the Atmospheric Sciences **54**(2), 286–313 (1997)
9. Frederolsem, J., Carnevale, G.: Stability properties of exact nonzonal solutions for flow over topography. Geophysical & Astrophysical Fluid Dynamics **35**(1-4), 173–207 (1986)
10. Gettelman, A., Kay, J., Shell, K.: The evolution of climate sensitivity and climate feedbacks in the community atmosphere model. Journal of Climate **25**(5), 1453–1469 (2012)
11. Harlim, J., Mahdi, A., Majda, A.J.: An ensemble Kalman filter for statistical estimation of physics constrained nonlinear regression models. Journal of Computational Physics **257**, 782–812 (2014)
12. Kalnay, E.: Atmospheric modeling, data assimilation and predictability. Cambridge university press (2003)
13. Kleeman, R., Majda, A.J., Timofeyev, I.: Quantifying predictability in a model with statistical features of the atmosphere. Proceedings of the National Academy of Sciences **99**(24), 15,291–15,296 (2002)
14. Kraichnan, R.H., Montgomery, D.: Two-dimensional turbulence. Reports on Progress in Physics **43**(5), 547–619 (1980)
15. Lesieur, M.: Turbulence in fluids, vol. 40. Springer Science & Business Media (2012)
16. Majda, A.: An introduction to turbulent dynamical systems in complex systems, *Frontiers in Applied Dynamical Systems: Reviews and Tutorials*, vol. 5, 1 edn. Springer International Publishing (2016)
17. Majda, A., Wang, X.: Nonlinear dynamics and statistical theories for basic geophysical flows. Cambridge University Press (2006)
18. Majda, A.J.: Statistical energy conservation principle for inhomogeneous turbulent dynamical systems. Proceedings of the National Academy of Sciences **112**(29), 8937–8941 (2015)
19. Majda, A.J., Qi, D.: Improving prediction skill of imperfect turbulent models through statistical response and information theory. Journal of Nonlinear Science **26**(1), 233–285 (2016)
20. Majda, A.J., Qi, D.: Strategies for reduced-order models for predicting the statistical responses and uncertainty quantification in complex turbulent dynamical systems. SIAM Review, in press (2017)

21. Majda, A.J., Qi, D.: Using statistical functionals for effective control of inhomogeneous complex turbulent dynamical systems. submitted to Physica D: Nonlinear Phenomena (2017)
22. Majda, A.J., Timofeyev, I., Vanden-Eijnden, E.: Systematic strategies for stochastic mode reduction in climate. Journal of the Atmospheric Sciences **60**(14), 1705–1722 (2003)
23. Majda, A.J., Tong, X.T.: Ergodicity of truncated stochastic Navier Stokes with deterministic forcing and dispersion. Journal of Nonlinear Science **26**(5), 1483–1506 (2016)
24. Palmer, T.N.: Predicting uncertainty in forecasts of weather and climate. Reports on progress in Physics **63**(2), 71–116 (2000)
25. Pedlosky, J.: Geophysical fluid dynamics. Springer Science & Business Media (2013)
26. Qi, D., Majda, A.J.: Low-dimensional reduced-order models for statistical response and uncertainty quantification: Two-layer baroclinic turbulence. Journal of the Atmospheric Sciences **73**(12), 4609–4639 (2016)
27. Qi, D., Majda, A.J.: Low-dimensional reduced-order models for statistical response and uncertainty quantification: Barotropic turbulence with topography. Physica D: Nonlinear Phenomena **343**, 7–27 (2017)
28. Salmon, R.: Lectures on geophysical fluid dynamics. Oxford University Press (1998)
29. Shepherd, T.G.: Rigorous bounds on the nonlinear saturation of instabilities to parallel shear flows. Journal of Fluid Mechanics **196**, 291–322 (1988)
30. Tracton, M.S., Kalnay, E.: Operational ensemble prediction at the national meteorological center: Practical aspects. Weather and Forecasting **8**(3), 379–398 (1993)